

FINITE-QUARK-MASS EFFECTS ON THE HIGGS PRODUCTION CROSS SECTION IN THE GLUON-GLUON FUSION CHANNEL

Dissertation

zur Erlangung des Doktorgrades an der Fakultät für Mathematik, Informatik und
Naturwissenschaften

Fachbereich Physik der Rheinisch-Westfälischen Technischen Hochschule

vorgelegt von

TOM CLAUS RUDOLF SCHELLENBERGER

Aachen

1. Juli 2025

Finite-Quark-Mass Effects on the Higgs Production Cross Section in the Gluon-Gluon Fusion Channel

© Tom Claus Rudolf Schellenberger 2025

GUTACHTER DER DISSERTATION:

Prof. Dr. Michał Czakon
Prof. Dr. Robert Harlander

ZUSAMMENSETZUNG DER PRÜFUNGSKOMMISSION:

Prof. Dr. Michał Czakon
Prof. Dr. Robert Harlander
TBA
TBA

VORSITZENDER DER PRÜFUNGSKOMMISSION:

TBA

DATUM DER DISPUTATION:

TBA

DEKAN DER FAKULTÄT MIN:

Prof. Dr. Carsten Honerkamp

ABSTRACT

This is my Abstract

ZUSAMMENFASSUNG

Dies ist meine Zusammenfassung

ACKNOWLEDGMENTS

Here is where I thank god.

PUBLICATIONS

During my PhD studies, I co-authored the following publications:

- [1] Michał Czakon, Felix Schlenker, and Tom Schellenberger. “Revisiting the double-soft asymptotics of one-loop amplitudes in massless QCD.” In: *JHEP* 04 (2023), p. 065. DOI: [10.1007/JHEP04\(2023\)065](#). arXiv: [2211.06465 \[hep-ph\]](#)
- [2] Michał Czakon, Felix Schlenker, and Tom Schellenberger. “Subleading effects in soft-gluon emission at one-loop in massless QCD.” In: *JHEP* 12 (2023), p. 126. DOI: [10.1007/JHEP12\(2023\)126](#). arXiv: [2307.02286 \[hep-ph\]](#)
- [3] Michał Czakon et al. “Top-Bottom Interference Contribution to Fully Inclusive Higgs Production.” In: *Phys. Rev. Lett.* 132.21 (2024), p. 211902. DOI: [10.1103/PhysRevLett.132.211902](#). arXiv: [2312.09896 \[hep-ph\]](#)
- [4] Michał Czakon et al. “Quark mass effects in Higgs production.” In: *JHEP* 10 (2024), p. 210. DOI: [10.1007/JHEP10\(2024\)210](#). arXiv: [2407.12413 \[hep-ph\]](#)

Among these, only the last two are directly relevant to this dissertation.

CONTENTS

1	Introduction	1
2	The Standard Model of Particle Physics	3
2.1	Electroweak Symmetry breaking	3
2.2	Cross Sections	7
2.2.1	The Hard Scattering Amplitude	8
2.2.2	The Parton Distribution Functions	11
2.2.3	The Phase-Space Integration	13
3	The Higgs as a Window to New Physics	19
3.1	Stability of the Higgs Potential	19
3.2	The Hierarchy Problem	19
4	Hadronic Higgs Production	21
4.1	Motivation (better title needed!)	21
4.2	The Leading-Order Cross Section	21
4.3	The Heavy-Top Limit	25
4.4	Higher-Order Corrections	29
4.5	Theory Status	29
5	Computational Details	31
5.1	Computing the Amplitudes	31
5.1.1	The Real-Real Corrections	31
5.1.2	The Real-Virtual Corrections	31
5.1.3	The Virtual-Virtual Corrections	31
5.2	$\overline{\text{MS}}$ -scheme	31
5.3	The 4-Flavour Scheme	31
5.4	Performing the Phase-Space Integration	31
6	Results and Discussion	33
6.1	Total Cross Section	33
6.1.1	Effects of Finite Top-Quark Masses	33
6.1.2	Effects of Finite Bottom-Quark Masses	33
6.2	Differential Cross Section	33
7	Conclusions	35
A	Feynman Rules of the Standard Model	37
	Bibliography	41

ACRONYMS

SM	Standard model
VEV	Vacuum expectation value
SSB	Spontaneous symmetry breaking
PDF	Parton distribution function
QCD	Quantum chromodynamics
RGE	Renormalization group equation
LO	Leading order
DR	Dimensional regularization
UV	Ultraviolet
IR	Infrared
LO	Leading order
NLO	Next-to-leading order
NNLO	Next-to-next-to-leading order
OS	On-shell renormalization
RG	Renormalization group
RGE	Renormalization group equation
LHC	Large hadron collider
FS	Flavor scheme
MC	Monte-Carlo
LME	Large mass expansion
HEL	High-energy limit
HTL	Heavy-top limit

NOTATION, CONSTANTS AND CONVENTIONS

- In this thesis, I will be using the *Einstein summation convention*, by which any index—be it a Lorentz, color or flavor index—which appears twice is implicitly summed over.
- I will be using natural units

$$\hbar = c = 1. \quad (0.1)$$

- The electron charge is

$$-e, \quad e > 0. \quad (0.2)$$

- The metric is

$$g_{\mu\nu} = \begin{pmatrix} 1 & & & \\ & -1 & & \\ & & -1 & \\ & & & -1 \end{pmatrix}. \quad (0.3)$$

- The normalization of the Levi-Civita anti-symmetric tensor $\epsilon_{\mu\nu\rho\sigma}$ is

$$\epsilon_{0123} = +1 \quad (0.4)$$

- The Pauli matrices are defined as

$$\sigma^1 \equiv \begin{pmatrix} 0 & 1 \\ 1 & 0 \end{pmatrix}, \quad \sigma^2 \equiv \begin{pmatrix} 0 & -i \\ i & 0 \end{pmatrix}, \quad \sigma^3 \equiv \begin{pmatrix} 1 & 0 \\ 0 & -1 \end{pmatrix}, \quad \tau^i \equiv \sigma^i. \quad (0.5)$$

- Unless specifically specified otherwise we will use the following values for appearing physical constants

- $G_F = 1.16637 \times 10^{-5} \text{ GeV}^{-2}$
- $m_H = 125.00 \text{ GeV}$
- $m_t = 173.06 \text{ GeV}$
- $\overline{m}_t(\overline{m}_t) = 162.7 \text{ GeV}$
- $m_b = 4.18 \text{ GeV}$
- $\overline{m}_b(\overline{m}_b) = 2.41 \text{ GeV}$
- $m_c = 1.27 \text{ GeV}$
- $m_Z = 91.1876 \text{ GeV}$

- We use the `NNPDF31_nnlo_as_0118` and `NNPDF31_nnlo_as_0118_nf_4PDF` set in the 5FS and 4FS respectively.

- α_s is extracted from the PDF set at the Z^0 mass.

1 | INTRODUCTION

General introductions

2.1 ELECTROWEAK SYMMETRY BREAKING

The standard model (SM) of particle physics is a theory describing all known matter and their fundamental interactions except for gravity. It unifies the electromagnetic, weak, and strong forces under a single theoretical framework. The matter content of the SM is classified into two primary groups: *fermions* and *bosons*. The fermions have spin 1/2, they are further subcategorized into *quarks* and *leptons*. Quarks participate in strong interactions, while leptons interact only via the electromagnetic and weak forces. In contrast, bosons have integer spin. There exists a single particle with spin 0, the *Higgs* boson, and four vector bosons, namely the gluon, the photon, and the *W* and *Z* boson. The vector bosons act as force carrier for the strong, the electromagnetic and the weak force respectively. Fermions are organized into three generations, with each generation containing two types of quarks (up-type and down-type) and two leptons (a charged lepton and its corresponding neutrino). These generations are shown in Fig. 2.1, along with their masses, charges, and spins.

The interactions between SM particles are described by a non-abelian gauge theory of the $SU(3)_C \times SU(2)_L \times U(1)_Y$ group. Here $SU(3)_C$ governs the strong interactions. It applies to all *colored* particles, i.e. quarks and gluons. The quarks transform under the fundamental representation of the $SU(3)_C$ group. $SU(2)_L \times U(1)_Y$ governs electroweak interactions. The $SU(2)_L$ transformation acts non-trivially only on *left-handed* fermions which form doublets

$$L_{iL} \equiv \begin{pmatrix} \nu_{iL} \\ l_{iL} \end{pmatrix}, \quad Q_{iL} \equiv \begin{pmatrix} u_{iL} \\ d_{iL} \end{pmatrix}, \quad (2.1)$$

$$\nu_i = (\nu_e, \nu_\mu, \nu_\tau), \quad l_i = (e, \mu, \tau), \quad u_i = (u, c, t), \quad d_i = (d, s, b).$$

The phase transformation $U(1)_Y$ acts on all particles except neutrinos according to their quantum number, the *hypercharge* Y . The symmetry is spontaneously broken to $SU(3)_C \times U(1)_Q$, where the $U(1)_Q$ group corresponds to gauge transformation of the electromagnetic interaction, hence the subscript Q for the *electric charge*. To ensure that the particles have the correct charges, the hypercharge must satisfy the *Gell-Mann–Nishijima relation*:

$$\frac{Y}{2} = Q - I^3. \quad (2.2)$$

With the particle charges displayed in Fig. 2.1 we then get

	L_{iL}	Q_{iL}	ν_{iR}	l_{iR}	u_{iR}	d_{iR}
$\frac{Y}{2}$	$-\frac{1}{2}$	$\frac{1}{6}$	0	-1	$\frac{2}{3}$	$-\frac{1}{3}$



Figure 2.1: Elementary particles of the SM. The was image generated with the help of Ref. [5].

The transformation properties of the gauge bosons is dictated by the covariance of the covariant derivative

$$D_\mu \equiv \partial_\mu - igA_\mu^a T_R^a - ig_2 W_\mu^a I^a + ig_Y \frac{Y}{2} B_\mu$$

$$T_R^a = \begin{cases} T^a & \text{for quarks,} \\ 0 & \text{for leptons,} \end{cases} \quad I^a = \begin{cases} \frac{\tau}{2} & \text{for left-handed fermions,} \\ 0 & \text{for right-handed fermions,} \end{cases} \quad (2.3)$$

where T^a and τ^a are the *Gell-Mann* and *Pauli* matrices.

Before spontaneous symmetry breaking, the Lagrangian which governs the evolution of all matter fields must be invariant under the $SU(3)_C \times SU(2)_L \times U(1)_Y$ gauge group. Up to a \mathbb{CP} violating term¹ the SM Lagrangian is the most general mass-dimension four Lagrangian for the described particle content

$$\mathcal{L}_{\text{SM}} = \mathcal{L}_G + \mathcal{L}_F + \mathcal{L}_Y + \mathcal{L}_H. \quad (2.4)$$

¹ The absence of the \mathbb{CP} violating term $\theta \frac{g^2}{64\pi^2} \epsilon^{\mu\nu\alpha\beta} F_{\mu\nu}^a F_{\alpha\beta}^a$ is an unsolved problem of particle physics, known as the strong CP problem.

The gauge-field Lagrangian \mathcal{L}_G describes the free propagation and in the case of the non-abelian groups $SU(3)_C$ and $SU(2)_L$ also the self-interaction of the gauge bosons. It is given by

$$\begin{aligned}\mathcal{L}_G &= -\frac{1}{4}G_{\mu\nu}^a G^{a\mu\nu} - \frac{1}{4}W_{\mu\nu}^a W^{a\mu\nu} - \frac{1}{4}B_{\mu\nu}B^{\mu\nu}, \\ G_{\mu\nu}^a &\equiv \partial_\mu A_\nu^a - \partial_\nu A_\mu^a + gf^{abc}A_\mu^b A_\nu^c, \\ W_{\mu\nu}^a &\equiv \partial_\mu W_\nu^a - \partial_\nu W_\mu^a + g_2\epsilon^{abc}W_\mu^b W_\nu^c, \\ B_{\mu\nu} &\equiv \partial_\mu B_\nu - \partial_\nu B_\mu.\end{aligned}\tag{2.5}$$

The propagation of the fermions and their interaction with the gauge bosons is described by

$$\mathcal{L}_F = \bar{L}_{iL}i\not{D}L_{iL} + \bar{\nu}_{iR}i\not{D}\nu_{iR} + \bar{l}_{iR}i\not{D}l_{iR} + \bar{Q}_{iL}i\not{D}Q_{iL} + \bar{u}_{iR}i\not{D}u_{iR} + \bar{d}_{iR}i\not{D}d_{iR}.\tag{2.6}$$

The Higgs field is a doublet of the $SU(2)_L$ group. We want the field to have a non-vanishing vacuum expectation value (VEV) to dynamically generate the fermion and boson masses. Of course, the vacuum cannot carry an electric charge, which means that the Higgs field must be electrically neutral along the direction of *spontaneous symmetry breaking* (SSB). We choose this to be the second component of the doublet. With the Gell-Mann–Nishijima relation we can then deduce that hypercharge of the doublet must be $Y = +1$. The Higgs doublet field thus takes the form

$$\Phi = \begin{pmatrix} \phi^+ \\ \phi^0 \end{pmatrix},\tag{2.7}$$

where the superscript indicates the electric charge.

In order to generate a non-vanishing VEV, the Higgs field must be in a potential with a global minimum away from zero. Hence, the only gauge invariant mass-dimension four Lagrangian we can construct is

$$\begin{aligned}\mathcal{L}_H &= (D_\mu\Phi)^\dagger (D^\mu\Phi) - V(\Phi) \\ V(\Phi) &= \lambda(\Phi^\dagger\Phi)^2 - \mu^2\Phi^\dagger\Phi, \quad \mu^2, \lambda > 0.\end{aligned}\tag{2.8}$$

The minimum of the Higgs potential V is at

$$\Phi_0^\dagger\Phi_0 = \frac{\mu^2}{2\lambda} \equiv \frac{v^2}{2} \neq 0.\tag{2.9}$$

After (SSB) we can expand the Higgs field around its minimum

$$\Phi = \begin{pmatrix} \phi^+ \\ \frac{1}{\sqrt{2}}(v + H + i\xi) \end{pmatrix}\tag{2.10}$$

The real scalar field H is the famous Higgs boson, whereas the fields ϕ^\pm and ξ are unphysical since they can always be eliminated through a gauge transformation (*would-be Goldstone bosons*). After inserting the expansion in the Higgs Lagrangian, the mass of the Higgs can be read off from its square term

$$m_H = \sqrt{2}\mu.\tag{2.11}$$

SSB enables the generation of vector boson masses without breaking the gauge symmetry explicitly. If we insert the expanded Higgs field in the Higgs Lagrangian, we get quadratic terms of the gauge boson fields

$$\begin{aligned}\mathcal{L}_H &\supseteq \frac{v^2}{2} \left\{ g_2^2 \begin{pmatrix} 0 & 1 \end{pmatrix} I^a I^b \begin{pmatrix} 0 \\ 1 \end{pmatrix} W_\mu^a W^{b\mu} - g_2 g_Y \begin{pmatrix} 0 & 1 \end{pmatrix} I^a \begin{pmatrix} 0 \\ 1 \end{pmatrix} W_\mu^a B^\mu + \frac{g_Y^2}{4} B_\mu B^\mu \right\} \\ &= \frac{v^2}{2} \left\{ \frac{g_2^2}{4} [(W^1)^2 + (W^2)^2] + \frac{1}{4} \begin{pmatrix} B^\mu & W^{3\mu} \end{pmatrix} \begin{pmatrix} g_Y^2 & g_Y g_2 \\ g_Y g_2 & g_2^2 \end{pmatrix} \begin{pmatrix} B_\mu \\ W_\mu^3 \end{pmatrix} \right\}.\end{aligned}\quad (2.12)$$

By diagonalizing the mass matrix we obtain the physical states

$$\begin{pmatrix} A_\mu^\gamma \\ Z_\mu \end{pmatrix} = \begin{pmatrix} \cos \theta_W & -\sin \theta_W \\ \sin \theta_W & \cos \theta_W \end{pmatrix} \begin{pmatrix} B_\mu \\ W_\mu^3 \end{pmatrix}, \quad \cos \theta_W = \frac{g_2}{\sqrt{g_Y^2 + g_2^2}}, \quad \sin \theta_W = \frac{g_Y}{\sqrt{g_Y^2 + g_2^2}}. \quad (2.13)$$

In this new basis, we have one massless boson A_μ^γ , which we identify as the photon and a charge neutral boson of mass

$$m_Z = \frac{v}{2} \sqrt{g_Y^2 + g_2^2}. \quad (2.14)$$

The vector bosons W^1 and W^2 are not eigenstates of the charge operator. We therefore define the new states

$$W_\mu^\pm = \frac{1}{\sqrt{2}} (W_\mu^1 \mp i W_\mu^2), \quad Q W_\mu^\pm = \pm W_\mu^\pm, \quad (2.15)$$

which are eigenstates of Q and have mass

$$m_W = \frac{v}{2} g_2. \quad (2.16)$$

Last but not least, we discuss the Yukawa sector of the SM Lagrangian. Before SSB, fermions cannot generate masses because a mass term would mix the left- and right-handed components of the fields, thereby breaking the chiral gauge symmetry. Here, once again, the Higgs field comes to the rescue: by coupling the fermions with the Higgs field through a Yukawa interaction²

$$\mathcal{L}_Y = - \left(y_{ij}^\nu \bar{L}_{iL} \Phi^c \nu_{jR} + y_{ij}^l \bar{L}_{iL} \Phi l_{jR} + y_{ij}^d \bar{Q}_{iL} \Phi d_{jR} + y_{ij}^u \bar{Q}_{iL} \Phi^c u_{jR} \right) + \text{h.c.}, \quad (2.17)$$

where Φ^c is the charge-conjugated field to Φ , we do not explicitly break the symmetry. However, after SSB this Lagrangian will generate exactly the required mixing between left- and right-handed fields to generate the fermion masses. The Yukawa-interaction matrices $y_{ij}^{\nu, l, d, u}$ can be shifted from the Yukawa sector to the fermion sector through a field redefinition. Indeed, if we apply the *singular value decomposition* of the Yukawa matrix

$$y = U_L^\dagger y_{\text{diag}} U_R, \quad \text{with} \quad (y_{\text{diag}})_{ij} = \sqrt{2} Y_i \delta_{ij} \quad \text{and} \quad U_{L,R} \in \text{U}(3), \quad (2.18)$$

and redefine our fermion fields to be

$$f_{iR} \longrightarrow U_{Rij} f_{jR}, \quad f_{iL} \longrightarrow U_{Lij} f_{jL}, \quad f = \nu, l, u, d \quad (2.19)$$

the Yukawa Lagrangian becomes

$$\mathcal{L}_Y = - \sum_i \left(m_{\nu_i} \bar{\nu}_i \nu_i + m_{l_i} \bar{l}_i l_i + m_{u_i} \bar{u}_i u_i + m_{d_i} \bar{d}_i d_i \right) \left(1 + \frac{H}{v} \right). \quad (2.20)$$

² In the original formulation of the SM, there are no neutrino Yukawa interactions, since they were believed to be massless. Neutrino oscillation experiments have shown however, that neutrinos do in fact have finite masses.

Here we identified the Yukawa coupling as $Y_i = m_i/v$ in order to generate the required mass terms. Consequently, we observe that the Yukawa coupling of the Higgs to the fermions is proportional to the mass of that fermion. The field redefinition is a change from a flavor eigenbasis, which is diagonal in the couplings to the gauge bosons, to a mass eigenbasis. In the mass eigenbasis the part of fermion Lagrangian which contains the interaction to the electroweak gauge bosons after SSB is

$$\begin{aligned} \mathcal{L}_F \supset & \sum_f (-Q_f) e \bar{f}_i \not{A} f_i + \sum_f \frac{e}{\sin \theta_W \cos \theta_W} \bar{f}_i (I_f^3 \gamma^\mu P_L - \sin^2 \theta_W Q_f \gamma^\mu) f_i Z_\mu \\ & + \frac{e}{\sqrt{2} \sin \theta_W} \left(\bar{u}_i \gamma^\mu P_L (V_{\text{CKM}})_{ij} d_j W_\mu^+ + \bar{d}_i \gamma^\mu P_L (V_{\text{CKM}}^\dagger)_{ij} u_j W_\mu^- \right) \\ & + \frac{e}{\sqrt{2} \sin \theta_W} \left(\bar{\nu}_i \gamma^\mu P_L (V_{\text{PMNS}}^\dagger)_{ij} l_j W_\mu^+ + \bar{l}_i \gamma^\mu P_L (V_{\text{PMNS}})_{ij} \nu_j W_\mu^- \right). \end{aligned} \quad (2.21)$$

Here we identified the electromagnetic coupling constant

$$e = \frac{g_2 g_Y}{\sqrt{g_2^2 + g_Y^2}}, \quad (2.22)$$

as the factor in front of the photon interaction term. The operators $P_{L,R}$ are just the projectors onto the left- and right-handed components

$$P_{L,R} = \frac{1 \mp \gamma^5}{2}. \quad (2.23)$$

The *CKM* and *PMNS matrices*³ are the results of the field redefinitions

$$V_{\text{CKM}} \equiv U_L^{u\dagger} U_L^d, \quad V_{\text{PMNS}} \equiv U_L^{l\dagger} U_L^\nu. \quad (2.24)$$

Typically, one prefers to work in the mass eigenbasis of the quarks, while the neutrinos are kept in the flavor eigenbasis, in which case one encounters flavor changes (*neutrino oscillations*) through propagation. This is why the PMNS matrix is defined in terms of the complex conjugate of the CKM matrix equivalent in the lepton sector.

2.2 CROSS SECTIONS

Cross sections offer the possibility to directly test the SM and many of the great successes of the SM are its *cross section* predictions. The cross section is simply defined as the probability to create some final state from some initial state per unit of time per target particle normalized by the incoming particle flux. This definition allows for straightforward measurement through counting experiments. For instance, experiments like **CMS** and **ATLAS** collide particles and count how often a particular final state is produced within a given time interval.

From a theoretical perspective, cross sections can be calculated using

$$d\sigma_{ij \rightarrow n} = \frac{1}{F} d\Phi_n |M_{ij \rightarrow n}|^2, \quad (2.25)$$

where F denotes the *flux factor*⁴

$$F \equiv 4p_1 \cdot p_2, \quad (2.26)$$

³ Named after Cabibbo, Kobayashi and Maskawa, and Pontecorvo, Maki, Nakagawa and Sakata.

⁴ In the following we assume that the initial state particles are massless.

$d\Phi_n$ is the *Lorentz invariant phase space measure*

$$d\Phi_n = \left[\prod_{i=1}^n \frac{d^4 q_i}{(2\pi)^4} (2\pi) \delta(q_i^2 - m_i^2) \Theta(q_i^0) \right] (2\pi)^4 \delta^{(4)} \left(p_1 + p_2 - \sum_{i=1}^n q_i \right), \quad (2.27)$$

and M_{fi} is the *scattering amplitude* describing the short distance interactions.

The computation of cross sections involves three basic steps:

1. Calculation of the hard scattering amplitude,
2. Phase-space integration,
3. And the convolution with *parton distribution functions* (PDFs).

We will discuss each step in detail below.

2.2.1 The Hard Scattering Amplitude

The Hard Scattering Amplitude describes the transition probability from a specific initial state to a particular final state. Since the scattering is **hard**, it implies that the energy transfer between particles during scattering is large compared to the QCD scale. Thus, we operate within the perturbative regime of QCD and can perform an expansion in terms of the coupling constant

$$M_{ij \rightarrow n} = \alpha_s^{n_{\text{Born}}} \left(M_{ij \rightarrow n}^{(0)} + \frac{\alpha_s}{\pi} M_{ij \rightarrow n}^{(1)} + \left(\frac{\alpha_s}{\pi} \right)^2 M_{ij \rightarrow n}^{(2)} + \mathcal{O}(\alpha_s^3) \right). \quad (2.28)$$

Here, n_{Born} denotes the power of the coupling constant at *leading order* (LO). The coefficients in this series can be computed graphically using *Feynman rules*. These are the set of all allowed propagators and vertices together with the corresponding mathematical prescription. The Feynman rules for the complete SM are listed in Appendix A. To calculate the coefficient $M_{ij \rightarrow n}^{(l)}$ for a specific process, one has to draw all possible connected and amputated Feynman diagrams with the initial state (i, j) and final state n , that contain $2(n_{\text{Born}} + l)$ vertices⁵. Then one uses the Feynman rules to get the mathematical translation, keeping in mind that momentum must be conserved at every vertex and also taking into account possible symmetry factors.

Starting from $M_{ij \rightarrow n}^{(1)}$, but for some processes, called *loop induced processes*, even from $M_{ij \rightarrow n}^{(0)}$, we will encounter loops in the diagrams. Inside a loop, the momentum of the edges cannot be uniquely determined through momentum conservation. Consequently, we must leave momentum unspecified and integrate over all possible values. Typically, it is the computation of these *loop integrals* that makes the calculation of hard scattering amplitudes so challenging. A plethora of powerful techniques has been developed over the years to tackle this daunting task. Still, the computation of loop integrals remains a highly active field of research and two-loop amplitudes with 5 or more scales are only just becoming available. A detailed description of modern techniques is beyond the scope of this thesis. For a comprehensive overview see Ref. [6].

Loop integrals are notorious for exhibiting divergences. To tame these, we introduce *regulators*, i.e. we introduce a parameter, such that the integral becomes function of that parameter with a singularity at the physical value. The most commonly used regularization scheme is

⁵ Quartic vertices are counted twice.

dimensional regularization (DR), here we make the loop-integral a function of the dimension by replacing

$$\int \frac{d^4k}{(2\pi)^4} (\dots) \longrightarrow \bar{\mu}^{2\epsilon} \int \frac{d^d k}{(2\pi)^d} (\dots), \quad d \equiv 4 - 2\epsilon \in \mathbb{C}, \quad \gamma_E = 0.5772 \dots \quad (2.29)$$

The dimensionally regularized integral satisfies the usual integral properties like linearity, translation invariance and rescaling. The mass scale,

$$\bar{\mu}^2 = \frac{\mu^2}{4\pi} e^{\gamma_E} \quad (2.30)$$

was introduced to retain the mass dimension of the measure to 4, while absorbing some common factors of loop integrals. The physical limit then corresponds to $\epsilon \rightarrow 0$. A divergent integral in four dimensions will hence have ϵ -poles in DR. The poles are categorized as *ultraviolet* poles if their origin are large loop momenta, i.e. the four dimensional integral diverges for $k \rightarrow \infty$. Further we categorize poles as *infrared* poles if the singularity arises from loop momenta which are either soft ($k \rightarrow 0$) or *collinear* ($k \cdot p_i \rightarrow 0$) to one of the external massless legs. UV and IR singularities are mutually exclusive since they originate from different regions of the phase space. This means that the poles do not multiply together, and we may only get a single UV pole per loop integration. The soft and collinear singularities are **not** exclusive, meaning that IR singularities can develop one double pole per loop integration.

The IR singularities cancel for inclusive observables as we shall discuss in detail in section 2.2.3. UV poles on the other hand, are removed through a method called *renormalization*. Renormalization hinges on the idea, that the fields, constants and masses we observe in nature are not necessarily the same as the one in our Lagrangian. Instead, they are related through a *renormalization constant*

$$\begin{aligned} W_\mu^{B,a} &= (Z_3^W)^{1/2} W_\mu^{R,a} \\ B_\mu^B &= (Z_3^Z)^{1/2} B_\mu^R \\ A_\mu^{B,a} &= (Z_3^A)^{1/2} A_\mu^{R,a} \\ \Phi^B &= (Z^\Phi)^{1/2} \Phi^R \\ Q_{iL}^B &= (Z_{2i}^L)^{1/2} Q_{iL}^R \\ u_{iR}^{B,a} &= (Z_{2i}^{u,R})^{1/2} u_{iR}^{B,a} \\ d_{iR}^{B,a} &= (Z_{2i}^{d,R})^{1/2} d_{iR}^{B,a} \\ g^B &= Z_g g^R \\ g_Y^B &= Z_Y g_Y^R \\ g_2^B &= Z_2 g_2^R \\ (\mu^2)^B &= Z_\mu (\mu^2)^R \\ \lambda^B &= Z_\lambda \lambda^R \\ y_{ij}^{d,B} &= Z_{y,ij}^d y_{ij}^{d,R} \\ y_{ij}^{u,B} &= Z_{y,ij}^u y_{ij}^{u,R} \end{aligned} \quad (2.31)$$

In these equations B refers to *bare* quantities appearing within our Lagrangian while R signifies renormalized quantities that are finite by definition. In the SM, it can be shown [7, 8] that we can choose renormalization constants, such that *Green's functions*, i.e. vacuum expectation values of time ordered products of local renormalized fields, are free of UV divergences. Scattering amplitudes, generally do not depend on the unphysical fields, which is why the fields can be kept unrenormalized in this case. Since at LO Green's functions do not require renormalization, all renormalization constants are equal to the identity at this order.

The definition of the renormalization constants is not unique. Indeed, the renormalization constants were designed to absorb singularities, but the finite part is a priori unconstrained. We call a prescription which uniquely determines the renormalization constants a *renormalization scheme*. The most widely used renormalization scheme is the $\overline{\text{MS}}$ scheme. Here, beyond the leading 1 and a universal factor of $\bar{\mu}^{\epsilon\rho_i}$, the renormalization constants **only** consist of poles, i.e. the renormalization constants have the structure

$$Z_i(\alpha) = \bar{\mu}^{\epsilon\rho_i} \left(1 + \frac{z_1}{\epsilon} \frac{\alpha}{4\pi} + \left(\frac{z_{22}}{\epsilon^2} + \frac{z_{21}}{\epsilon} \right) \left(\frac{\alpha}{4\pi} \right)^2 + \dots \right). \quad (2.32)$$

ρ_i is the mass dimension of the operator in units of ϵ , so that the factor $\bar{\mu}^{\epsilon\rho_i}$ corrects for the mismatch in mass dimensions between the four-dimensional renormalized and the d -dimensional bare quantities. For example: the coupling constant g^B has mass dimension ϵ , hence the renormalized coupling g^R has mass dimension zero and $\rho_i = 1$.

$\overline{\text{MS}}$ -renormalized masses are generally different from the pole mass. The *on-shell renormalization* (OS) scheme, is an alternative to the $\overline{\text{MS}}$ scheme specifically designed, such that the renormalized mass matches the pole mass. It is therefore the suitable choice for external particles that are asymptotically free. Bare quantities are independent of the chosen renormalization scheme. The invariance under the change of the renormalization scheme defines a group, the *renormalization group* (RG). In the $\overline{\text{MS}}$ scheme, the change from one scale $\bar{\mu}$ to another defines a continuous subgroup of the RG. This means we can formulate the invariance in terms of a differential equation

$$0 = \frac{d}{d \log \mu} a^B = a^R \frac{dZ_a^{\overline{\text{MS}}}}{d \log \mu} + Z_a^{\overline{\text{MS}}} \frac{da^R}{d \log \mu}, \quad (2.33)$$

where a could be a mass or a coupling. Eq. (2.33) is called the *renormalization group equation* (RGE) and it can be leveraged to determine the scale dependence, also called the *running*, of the observable.

The final step in calculating the hard scattering amplitude involves the application of the *Lehmann-Symanzik-Zimmermann* (LSZ) reduction formula. It relates the scattering amplitudes to Green's functions, and it is the reason why we only considered amputated Feynman diagrams. In practice, one just has to multiply each external field with the square root of the corresponding LSZ constant. These constants are defined as the proportionality factor between the propagator of the interacting and the free theory⁶. As such, they are numerically identical to the OS field renormalization constants.

⁶ The interacting field theory might have an additional continuous spectrum.

2.2.2 The Parton Distribution Functions

In hadron collisions, the initial state is not made up of elementary particles, but are bound states thereof. This means that during an inelastic scattering event, the partons which take part in the short-range interaction only carry a fraction of the original hadron momentum

$$p_1 = x_1 P_1, \quad p_2 = x_2 P_2. \quad (2.34)$$

Here p_1 and p_2 denote the momenta of the partons and P_1 and P_2 are the momenta of the hadrons. Since the momentum of the parton can not be larger than that of the hadron, $x_{1,2}$ is restricted to be less than one. Furthermore, since the energy of the parton must be positive the momentum fraction must also be positive. Otherwise, the momentum fraction is a priori unconstrained, we therefore integrate over all allowed values of x_1 and x_2

$$\begin{aligned} d\sigma_{H_1 H_2 \rightarrow n}(S) &= \int_0^1 dx_1 dx_2 f_{H_1,i}(x_1) f_{H_2,j}(x_2) d\hat{\sigma}_{ij \rightarrow n}(x_1 P_1, x_2 P_2, \mu_R) \\ &= \int_0^1 \frac{d\tau}{\tau} \mathcal{L}_{ij}(\tau) d\hat{\sigma}_{ij \rightarrow n}(\tau S, \mu_R) \end{aligned} \quad (2.35)$$

where $S = 2P_1 \cdot P_2$ is hadronic center of mass energy. $f_{H_k,i}(x_k)$ are the (unrenormalized) *parton distribution functions* (PDFs). They describe the probability of finding a parton i with momentum fraction x_k inside the hadron H_k . Lorentz invariance of the partonic cross section allowed us to conclude that it can only depend on the partonic center of mass energy \hat{s}

$$d\hat{\sigma}_{ij \rightarrow n}(x_1 P_1, x_2 P_2, \mu_R) = d\hat{\sigma}_{ij \rightarrow n}(x_1 x_2 S, \mu_R). \quad (2.36)$$

We then defined the *partonic luminosity*

$$\mathcal{L}_{ij}(\tau) \equiv (\tilde{f}_{H_1,i} \otimes \tilde{f}_{H_2,j})(\tau) \equiv \int_0^1 dx_1 dx_2 \tilde{f}_{H_1,i}(x_1) \tilde{f}_{H_2,j}(x_2) \delta(\tau - x_1 x_2), \quad (2.37)$$

where $\tilde{f}_{H,i}(x) \equiv x f_{H,i}(x)$, to arrive at the second line of Eq. (2.35).

At this stage the partonic cross section can still exhibit singularities whenever a final state parton becomes collinear to one of the initial state partons. At LO for example, the divergence due to initial-state collinear emissions reads

$$d\hat{\sigma}_{ab \rightarrow cX}(s, \mu_R) \Big|_{\text{div.}} = -\frac{\alpha_s}{2\pi} \frac{1}{\epsilon} \int_0^1 dz \left(P_{db}^{(0)}(z) d\hat{\sigma}_{ad \rightarrow X}(zs, \mu_R) + P_{da}^{(0)}(z) d\hat{\sigma}_{db \rightarrow X}(zs, \mu_R) \right), \quad (2.38)$$

where $P_{ij}^{(0)}$ are the LO *Altarelli-Parisi splitting kernels*.

We absorb these collinear singularities into the PDFs through a process called *collinear renormalization*, by defining the renormalized PDFs $f_{H,i}(x, \mu_F)$ via

$$f_{H,i}(x) \equiv (Z_{ij}(\cdot, \mu_F) \otimes f_{H,j}(\cdot, \mu_F))(x). \quad (2.39)$$

Beyond the pole term, the renormalization constants are generally scheme dependent. From Eq. (2.38) we see that the $\overline{\text{MS}}$ renormalization constant at NLO are given by

$$Z_{ij}(z, \mu_R, \mu_F) = \delta(1-z) \delta_{ij} + \frac{\alpha_s}{2\pi} \frac{1}{\epsilon} P_{ij}^{(0)}(z) + \mathcal{O}(\alpha_s^2). \quad (2.40)$$

Now the sum

$$d\sigma_{H_1 H_2 \rightarrow cX} + d\sigma_{H_1 H_2 \rightarrow X} \quad (2.41)$$

is guaranteed to be free initial-state collinear divergences.

Since the initial state collinear divergences are of a completely different origin than the UV divergences, we introduce a new scale μ_F , called the factorization scale. This scale separates the long-distance (non-perturbative) physics, contained in the PDFs, from the short-distance (perturbative) physics, contained in the partonic cross sections.

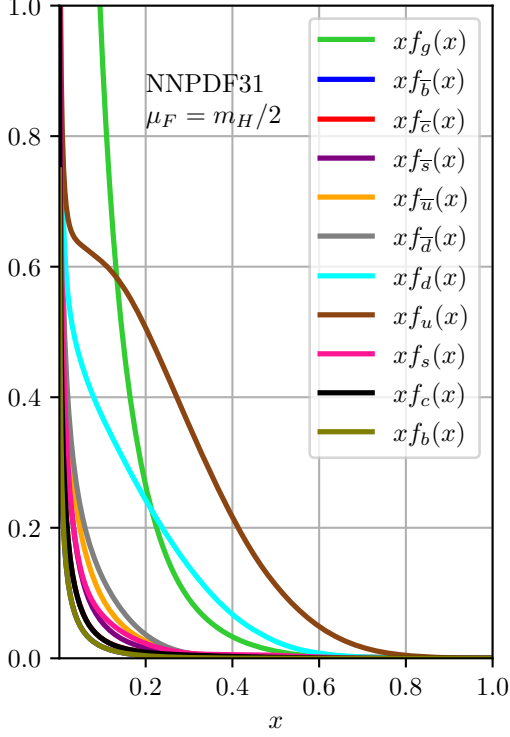


Figure 2.2: The various PDFs multiplied by x as a function of x . The plot was created using the LHAPDF6 [9] interface to the NNPDF31_nnlo_as_0118 [10] PDF set at a scale of $\mu_F = m_H/2$.

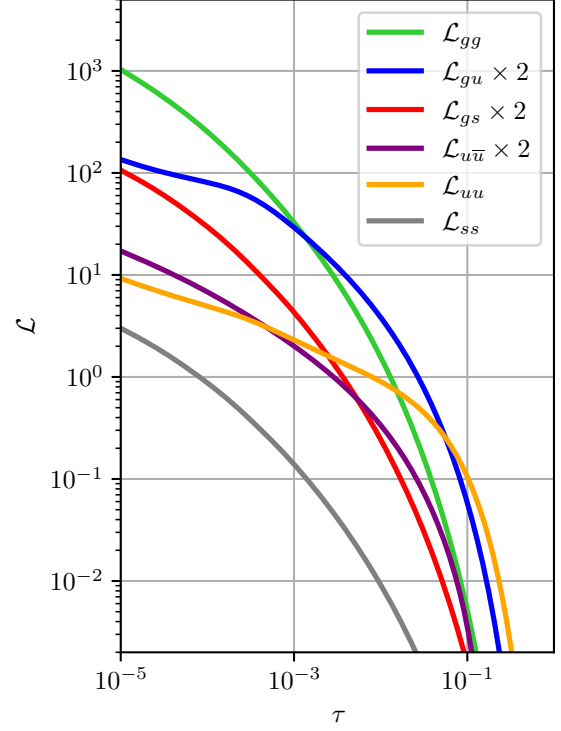


Figure 2.3: Partonic luminosity of parton i and j . We choose exemplary parton combinations to represent gluon-gluon, gluon-valence-quark, gluon-sea-quark, valence-quark-sea-quark, valence-quark-valence-quark and sea-quark-sea-quark luminosities. For the luminosity of two different partons we include a factor 2 to account for the different flavor permutations. The setup is the same as in Fig. 2.2.

The factorization theorem (2.35) is central in the SM as it tells us that the PDFs are universal quantities, i.e. they are not specific to any one process. It is a postulate of the parton model, in which hadrons are thought of as collection of the free elementary particles. In QCD however, the theorem requires proof [11]! The PDF for all light partons are displayed in Fig. 2.2. In Fig. 2.3 we show the partonic luminosity for exemplary parton combinations. PDFs describe long range interactions, a regime in which QCD is non-perturbative. As such, PDFs are non-perturbative objects which have to be measured in experiments or be calculated non-perturbatively, e.g. on the lattice.

The factorization scale is unphysical in the sense that it is not a parameter in our theory, nor can it be measured in an experiment. As usual we can apply the RGE to determine the running of the renormalized PDFs

$$0 = \frac{d}{d \ln \mu_F} f_{H,i}(x) = \frac{d}{d \ln \mu_F} (Z_{ij} \otimes f_{H,j}(\cdot, \mu_F))(x). \quad (2.42)$$

This can be rewritten to

$$\begin{aligned} \frac{d f_{H,i}(x, \mu_F)}{d \ln \mu_F} &= 2\alpha_s \left(Z_{ij}^{-1} \otimes \frac{d Z_{jk}^{(1)}}{d \alpha_s} \otimes f_{H,k}(\cdot, \mu_F) \right) (x, \mu_F) \\ &= \frac{\alpha_s}{\pi} \left(P_{ij}^{(0)} \otimes f_{H,j}(\cdot, \mu_F) \right) (x) + \mathcal{O}(\alpha_s^2), \end{aligned} \quad (2.43)$$

where $Z_{ij}^{(1)}$ is the residue of the renormalization constant. So even though the PDFs are non-perturbative, their dependence on the factorization scale is. Eq. (2.43) is the famous *Dokshitzer-Gribov-Lipatow-Altarelli-Parisi-evolution equation* (DGLAP equations) [12, 13, 14].

In the derivation above, we have treated the partons inside the hadrons as massless, which leads to real collinear singularities. In reality, all quarks have finite masses, so the phase-space integration only yields logarithmic mass enhancements of the form $\ln(\hat{s}/m_q^2)$ instead of actual singularities. The DGLAP equations then automatically resum these logarithms. For most applications at the LHC, the typical hard scattering scale is orders of magnitudes larger than all quark masses except for the top quark mass. It is therefore beneficial to treat them as massless partons, as the appearance of the large logarithms would otherwise completely destroy the perturbative convergence. However, treating quarks as massless also implies that we neglect their mass-dependent effects in the hard-scattering matrix elements. If the scattering process is sensitive to the quark masses—for example, in processes involving Higgs couplings to quarks—these mass effects might be lost.

The number of quark flavors treated as active (massless) partons defines our *flavor scheme* (FS). For instance, if we treat the lightest four flavors (up, down, strange, charm) as massless, while considering the bottom and top quarks as massive, we are working in the 4FS. Analogously, if the bottom quark is also considered massless, we are working in the 5FS, and so on.

2.2.3 The Phase-Space Integration

Even after renormalization and collinear renormalization can the amplitude exhibit divergences. The scattering amplitude in and of itself is not a physical observable; therefore, it is not required to be finite. Physical observables are cross sections, which are obtained by performing phase-space integrations over the squared amplitudes. However, even after integrating over the phase space, the cross section is not guaranteed to be finite. The reason is that the Born process is indistinguishable from processes with additional infrared radiation. Indeed, no matter how precise a detector is, below a certain resolution, it becomes impossible to detect a very soft photon or to distinguish two highly collinear jets. Hence, computing a cross section with a fixed final state does not make physical sense. Instead, one must consider sufficiently inclusive observables—so called *IR-safe observables*. For these, Kinoshita, Lee and Nauenberg proved that in unitary theories all IR singularities cancel [15, 16]. This is known as the Kinoshita-Lee-Nauenberg (KLN) theorem.

An example of an observable which is trivially IR safe is the fully inclusive cross section

$$\hat{\sigma}_{ij \rightarrow n+X} = \sum_{k=1}^{\infty} \hat{\sigma}_{ij \rightarrow n+k}, \quad \text{for } \hat{\sigma}_{ij \rightarrow n}^{(0)} \text{ finite,} \quad (2.44)$$

where $n+k$ indicates that in addition to the final state n we now have k massless partons of whatever flavor. In perturbation theory, the infinite sum is truncated at a given order and at each order

$$\hat{\sigma}_{ij \rightarrow n+X}^{(l)} = \sum_{k=0}^l \hat{\sigma}_{ij \rightarrow n+k}^{(l-k)}, \quad (2.45)$$

summed together with the contribution from collinear renormalization will be finite. For example at NLO, the finite inclusive cross section reads

$$\hat{\sigma}_{ij \rightarrow n+X}^{(1)} = \hat{\sigma}_{ij \rightarrow n}^R + \hat{\sigma}_{ij \rightarrow n}^V + \hat{\sigma}_{ij \rightarrow n}^C, \quad (2.46)$$

where

$$\hat{\sigma}_{ij \rightarrow n}^R = \frac{1}{F} \int d\Phi_{n+1} \sum_c |M_{ij \rightarrow n+c}^{(0)}|^2 \quad (2.47)$$

is the real correction,

$$\hat{\sigma}_{ij \rightarrow n}^V = \frac{1}{F} \int d\Phi_n 2\text{Re} \left(\left(M_{ij \rightarrow n}^{(0)} \right)^* M_{ij \rightarrow n}^{(1)} \right) \quad (2.48)$$

is the virtual correction, and

$$\hat{\sigma}_{ij \rightarrow n}^C = \frac{1}{F} \int d\Phi_n \frac{\alpha_s}{2\pi} \frac{1}{\epsilon} \left(\frac{\mu_R^2}{\mu_F^2} \right)^\epsilon \sum_c \int_0^1 dz \left[P_{ci}^{(0)}(z) |M_{cj \rightarrow n}^{(0)}|^2 + P_{cj}^{(0)}(z) |M_{ic \rightarrow n}^{(0)}|^2 \right] \quad (2.49)$$

are the corrections from collinear renormalization. Figure 2.4 provides a pictorial representation of the required partonic cross sections for Higgs boson production in the gluon fusion channel at various perturbative orders.

Although the sum of the contributions to the cross section is guaranteed to be finite due to the KLN theorem, the presence of IR singularities in individual terms poses significant challenges for practical calculations. These singularities prevent a straightforward evaluation of the phase-space integrals. To overcome this, we once again have to introduce regulators (such as dimensional regularization) to make the integrals well-defined. Over the years, numerous techniques have been developed to compute phase-space integrals efficiently. These techniques can generally be categorized into two main types: *Analytic methods*, and *numerical methods*.

As the name suggests, in the former class, the phase-space integrals are solved analytically. One noteworthy member of this class is the *reverse-unitarity method* [17], which was first applied to Higgs production in the gluon fusion channel. The method uses unitarity, to rewrite the phase-space integrals in terms of loop integrals over cut-propagators. One can then apply the remarkable techniques developed for Feynman integrals to these phase-space integrals and solve them analytically. The mayor downside of this approach is that it is highly process and observable dependent, meaning that for every process and every observable we have to start over from scratch. Furthermore, by the very nature of the method, you are always restricted to inclusive jet observables. Nevertheless, it has been successfully applied to, among others, Higgs-rapidity and Higgs- p_T distributions [18].



Figure 2.4: Pictorial representation of the needed partonic cross sections at various perturbative orders of the fully inclusive hadronic cross section. The graphic shows the example of Higgs production in the gluon fusion channel.

Among the numerical methods, there are two mayor approaches: *slicing* and *subtraction methods*. The former rely on a variable that isolates the IR-sensitive region of the phase space. Consider once again the example of Higgs production. Here, the IR-sensitive region of the phase space corresponds to configurations where the transverse momentum of the Higgs boson, p_T , approaches zero. The phase-space integral can then be decomposed into

$$\int_0^{p_T} dk_T d\hat{\sigma}_{ij \rightarrow H+c} = \int_0^{p_T^{\text{cut}}} dk_T d\hat{\sigma}_{ij \rightarrow H+c} + \int_{p_T^{\text{cut}}}^{p_T} dk_T d\hat{\sigma}_{ij \rightarrow H+c}. \quad (2.50)$$

The first integral on the right-hand side is now finite and can be computed numerically, e.g. using *Monte-Carlo* (MC) techniques. If we choose p_T^{cut} small enough, then we can approximate the integrand in the second integral, by its IR limit and solve the integral analytically. The pole of the integral should then cancel against the poles in the virtual integration and the counter term from collinear renormalization. The mayor advantage of this method is its simplicity. One big downside is its dependence on the unphysical cutoff scale. Ideally it is chosen very small, such that the approximation introduces little to no error. But if chosen too small, the integrations will have huge logarithmic enhancements which can easily spoil the numerical precision. Another disadvantage is that not all processes or observables have easily identifiable slicing variables, or the analytic integration is very challenging. For example, p_T slicing only works for color singlet production, indeed if we have a jet in the final state, we can encounter

collinear divergences also at finite transverse momenta of the jet. For processes involving jets, a possible slicing variable is the N -jettiness

$$\mathcal{T}_N \equiv \sum_k \min_i \left\{ \frac{2p_i \cdot q_k}{Q_i} \right\}, \quad (2.51)$$

with N , the number of jets, q_k , the momenta of the unresolved partons, p_i , the momenta of the resolved jets, and Q_i a normalization factor which can for example be set to the jet energy. However, the analytic integration becomes highly non-trivial and is a matter of active research. Currently, the N -jettiness beam functions are known at N³LO [19], the 0-jettiness soft function is known at N³LO [20, 21] and NNLO 1-jettiness soft functions and jet functions are also known [22, 23, 24, 25].

Subtraction methods on the other hand, work by subtracting the infrared limits at the integrand level. In the *Frixione-Kunszt-Signer subtraction scheme* (FKS subtraction scheme) one first isolates the IR divergence by partitioning the phase space into *sectors* using *selector functions*. These functions isolate specific infrared limits by approaching unity when a particular limit is approached (e.g., when an unresolved parton becomes soft or collinear) and vanish in other limits. For a single unresolved parton, a possible selector function is

$$\mathcal{S}_{n+1,k} \equiv \frac{1}{d_{n+1,k}} \left(\sum_k \frac{1}{d_{n+1,k}} \right)^{-1}, \quad \text{where} \quad d_{n+1,k} \equiv \left(\frac{E_{n+1}}{\sqrt{s}} \right)^\alpha (1 - \cos \theta_{n+1,k})^\beta. \quad (2.52)$$

The first index $n+1$ is the index of the unresolved parton, while the second index is the index of the reference parton. E_{n+1} denotes the energy of the unresolved parton, this factor is therefore to identify soft singularities. Consequently, the power α can be set to zero if the unresolved parton is a quark. Other than that, the powers must be strictly positive $\alpha, \beta > 0$. If $n+1$ now becomes collinear to one of the partons, say parton i , then the selector function $\mathcal{S}_{n+1,i}$ will approach one. And since the selector functions are strictly positive and form a decomposition of unity

$$\sum_k \mathcal{S}_{n+1,k} = 1, \quad (2.53)$$

all other selector functions will go to zero simultaneously.

The real emission cross section can then be written as a sum over sectors:

$$\hat{\sigma}_{ij \rightarrow n+u} = \frac{1}{F} \sum_k \int d\Phi_{n+1} |M_{ij \rightarrow n+u}^{(0)}|^2 \mathcal{S}_{n+1,k}. \quad (2.54)$$

Now say we found a way to factorize the phase space, such that the infrared limits of a specific sector, are isolated (see for example Ref. [26]). Then in each sector, we will have two unit integrations over ξ and η which parameterize the soft and collinear limit respectively, i.e. if $\xi \rightarrow 0$, then the momentum of the unresolved parton goes to zero and if $\eta \rightarrow 0$, the unresolved parton will become collinear to the reference momentum of that sector. The amplitude has the singular scaling $|M_{ij \rightarrow n+u}^{(0)}|^2 \sim \xi^{-2} \eta^{-1}$, leading to an integral of the form

$$\int_0^1 \frac{d\eta}{\eta^{1+\epsilon}} \frac{d\xi}{\xi^{1+2\epsilon}} f(\eta, \xi, \dots), \quad (2.55)$$

where f is a function regular in the limits $\eta, \xi \rightarrow 0$. If we now apply the distributional identity

$$\frac{1}{x^{1+\epsilon}} = \frac{1}{\epsilon} \delta(x) + \sum_{k=0} \frac{\epsilon^k}{k!} \left(\frac{\ln^k x}{x} \right)_+, \quad (2.56)$$

we can explicitly carry out all integrations.

The *sector improved residue subtraction scheme* [27] extends the FKS subtraction scheme to NNLO. As of today, it is the only subtraction scheme capable of computing any QCD phase-space integral. Beyond NNLO, developing efficient and general subtraction schemes remains an open challenge in perturbative QCD.

3 | THE HIGGS AS A WINDOW TO NEW PHYSICS

3.1 STABILITY OF THE HIGGS POTENTIAL

3.2 THE HIERARCHY PROBLEM

4

HADRONIC HIGGS PRODUCTION

4.1 MOTIVATION (BETTER TITLE NEEDED!)

Here I list various application for the Higgs production cross section and explain why precise predictions are so central. Maybe just put this in the chapter description?

4.2 THE LEADING-ORDER CROSS SECTION

Having established, that the gluon-fusion Higgs production cross section is central for many phenomenological applications, we now want to perform the actual LO calculation, which was first demonstrated by Georgi et al. in 1978 [28]. The calculation not only serves as an instructive example on cross section calculation, and thereby allows us to put our experience from section 2.2 to good use, but it already introduces many important concepts we can transfer to the NNLO computation.

At LO, there are only two possible Feynman diagrams we can draw. They are depicted in Fig. 4.1. As we can see. Gluon-fusion is a loop induced process with two scales: the mass of

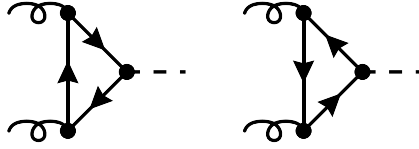


Figure 4.1: LO Feynman diagrams for Higgs production in the gluon-fusion channel.

the quark running in the loop m_q , and the Higgs mass m_H which must simultaneously be the partonic center of mass energy. The initial state gluons carry on the on-shell momenta p_1 and p_2 . Let us then define

$$i\mathcal{M} = i\mathcal{M}^{\mu\nu,ab}\varepsilon_\mu^a(p_1)\varepsilon_\nu^b(p_2). \quad (4.1)$$

With the Feynman rules presented in appendix A we find

$$\begin{aligned} i\mathcal{M}^{\mu\nu,ab} = & - \int \frac{d^4k}{(2\pi)^4} \\ & \times \text{Tr} \left[\frac{-im_q}{v} \delta_{ij} \frac{i(\not{k} + \not{p}_1 + \not{p}_2 + m_q)}{(k + p_1 + p_2)^2 - m_q^2} (ig\gamma^\nu T_{ik}^a) \frac{i(\not{k} + \not{p}_1 + m_q)}{(k + p_1)^2 - m_q^2} (ig\gamma^\mu T_{kj}^b) \frac{i(\not{k} + m_q)}{k^2 - m_q^2} \right] \\ & + \{p_1 \longleftrightarrow p_2, \mu \longleftrightarrow \nu, a \longleftrightarrow b\}, \end{aligned} \quad (4.2)$$

where the extra minus sign in front stems from the fermion trace.

Even without performing the explicit calculation can we already anticipate the general structure of the amplitude. Color wise, the amplitude must be proportional to δ^{ab} , because it is the

only available rank-two tensor. Since it is symmetric, the Lorentz structure must also be symmetric in order to satisfy *Bose symmetry*. The only building blocks we have available are $g^{\mu\nu}$, $(p_1^\mu p_2^\nu + p_2^\mu p_1^\nu)$, $p_1^\mu p_1^\nu$, and $p_2^\mu p_2^\nu$, but since all transverse parts drop out of the physical amplitude, the relevant tensors are only $g^{\mu\nu}$ and $p_2^\mu p_1^\nu$. Lastly, we know that the amplitude must satisfy the *Ward identity*, which allows us to restrict the tensor even further, such that we end up with

$$i\mathcal{M}^{\mu\nu,ab} = i\frac{\alpha_s}{\pi}\frac{1}{v}\delta^{ab}(p_2^\mu p_1^\nu - (p_1 \cdot p_2)g^{\mu\nu})\mathcal{C}(m_H, m_q). \quad (4.3)$$

Notice that we have only made use of very general properties of the amplitude. This is why the decomposition in Eq. (4.3) will hold at every order of α_s . The function $\mathcal{C}(m_H, m_q)$ is called the *Higgs-gluon form factor*. It has mass dimension 0, i.e. its functional dependence on m_q and m_H must be through a mass ratio

$$\mathcal{C}(m_H, m_q) = \mathcal{C}(z), \quad \text{with} \quad z \equiv \frac{m_H^2}{4m_q^2}. \quad (4.4)$$

The factor of $1/4$ was introduced, so that the *normal threshold* is located at $z = 1$. Mathematically, this means that $z = 1$ is a solution of the *Landau equations*. Physically, we can interpret the singularity as the point where we have enough energy to produce the quark pair on-shell. We can now project onto the form factor with

$$\mathcal{C}(z) = \frac{\pi v}{i\alpha_s N_c} \delta^{ab} \frac{1}{(p_1 \cdot p_2)^2 (d-2)} (p_2^\mu p_1^\nu - (p_1 \cdot p_2)g_{\mu\nu}) i\mathcal{M}^{\mu\nu,ab}. \quad (4.5)$$

If we now insert the LO expression of Eq. (4.2) and perform some basic manipulations we find

$$\begin{aligned} \mathcal{C}^{(0)}(z) = T_F \frac{1}{2-2\epsilon} \frac{1}{z} \int \frac{d^d k}{i\pi^{d/2}} \frac{1}{[k^2 - m_q^2 + i0^+][(k + p_1 + p_2)^2 - m_q^2 + i0^+]} \\ \times \left(2\epsilon + \frac{m_H^2}{[(k + p_1)^2 - m_q^2 + i0^+]} \left(\frac{1}{z} + \epsilon - 1 \right) \right), \end{aligned} \quad (4.6)$$

which, after inserting integrals and expanding in ϵ , finally reduces to

$$\mathcal{C}^{(0)}(z) = T_F \frac{1}{z} \left\{ 1 - \left(1 - \frac{1}{z} \right) \left[\frac{1}{2} \ln \left(\frac{\sqrt{1-1/z} - 1}{\sqrt{1-1/z} + 1} \right) \right]^2 \right\}. \quad (4.7)$$

We see that the Higgs-gluon form factor is roughly proportional to the square of the mass of the quark running in the loop. One power of m_q is hereby picked up from the Yukawa coupling. The other factor m_q is a consequence of the scalar coupling to Higgs. Indeed, without the quark mass, the trace in Eq. (4.2) would contain an odd number of gamma matrices and vanish consequently. Physically, we can interpret this as a helicity flip of the internal quark at the Higgs interaction vertex. And since massless QCD conserves helicity, the other helicity flip is provided by the mass. Similarly, since the two incoming gluons are vector bosons which should form a spinless final state, we would expect them to always carry opposite spins. This intuition is indeed confirmed by the tensor structure of the amplitude (4.3), as it always vanishes once contracted with two polarization vectors of the same helicity¹.

The LO Higgs-gluon form factor is plotted in Fig. 4.2. As expected, we pick up an imaginary part starting from the normal threshold at $z = 1$. If we expand the form factor around large

1 This can be seen easily by boosting to the center of mass frame and using $\epsilon^\mu(-\mathbf{p}, \lambda) \propto \epsilon^\mu(\mathbf{p}, -\lambda)$.

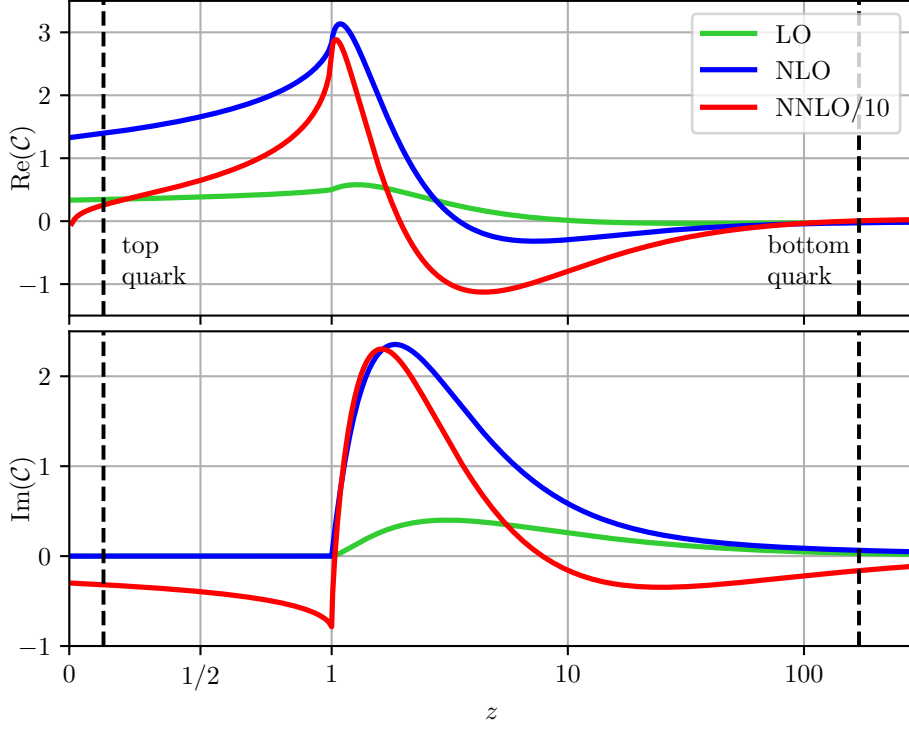


Figure 4.2: Real and imaginary part of the finite part of the Higgs-gluon form factor at various perturbative orders. NNLO is divided by ten for better visibility. NNLO results also depend on the number of light quark flavors, which has been set to 5 (5FS). Vertical lines indicate the z values for the top and bottom quark masses. The plot was created using the results of Ref. [29].

quark masses, i.e. we perform a *large mass expansion* (LME), we find that it approaches a constant

$$\mathcal{C}^{(0)}(z) = T_F \left(\frac{2}{3} + \frac{7}{45}z + \frac{4}{63}z^2 + \mathcal{O}(z^3) \right). \quad (4.8)$$

We will discuss the infinite mass limit in more detail in section 4.3. On the other side of the spectrum we can see that if the mass of the Higgs is far greater than the mass the internal quark, the form factor is approximately

$$\mathcal{C}^{(0)}(z) = \frac{T_F}{4z} \left[4 - \log^2(-4z) + \frac{1}{z} (\log(-4z) + \log^2(-4z)) + \mathcal{O}(1/z^2) \right]. \quad (4.9)$$

This expansion is known as *high-energy limit* HEL. The appearing double logarithms $\log^2(m_q^2/m_H^2)$ originate from a soft quark exchange. In fact, the quark mass acts as an infrared regulator of the integral in Eq. 4.6, so the appearance of these logarithms is not entirely unexpected. Numerically, these logarithms can be very large. The bottom quark, for example will yield a double logarithm of about 46. I.e., although suppressed by a factor of m_q^2/m_H^2 , the contributions from lighter quark flavors are logarithmically enhanced and hence highly significant for precision predictions.

If we now apply Eq. (2.25) and perform the phase space integration, which for a single particle is trivial because of the momentum conserving delta function, we get for the partonic cross section

$$\hat{\sigma}_{gg \rightarrow H}(\tau S) = \frac{\pi}{64v^2} m_H^2 \left(\frac{\alpha_s}{\pi} \right)^2 |\mathcal{C}(z)|^2 \delta(\tau S - m_H^2). \quad (4.10)$$

The initial state was averaged over spin and color. Finally, after the convolution with the partonic luminosity we arrive at the LO cross section

$$\sigma_{ggH}^{\text{LO}}(S) = \frac{\pi}{64v^2} \left(\frac{\alpha_s}{\pi} \right)^2 \mathcal{L}_{gg} \left(\frac{m_H^2}{S} \right) |\mathcal{C}^{(0)}(z)|^2. \quad (4.11)$$

From Fig. 4.2 we can see that the top quark exerts the largest impact on the Higgs-gluon form factor and hence the LO hadron cross section. We can read off the partonic luminosity from Fig. 2.3 and find that the cross section for the top quark induces Higgs production reads²

$$\sigma_{ggH}^{\text{LO}}(t) = 16.30 \text{ GeV} \quad (4.12)$$

at a hadronic center of mass energy of 13 TeV. Although expected to have little impact, we can also include the effects of finite bottom quark masses by coherently summing together the corresponding form factors. We find

$$\sigma_{ggH}^{\text{LO}}(t + b) = 14.72 \text{ GeV}, \quad (4.13)$$

i.e. the bottom quark lowers the cross section by around 9% at LO.

Without the inclusion of electro-weak corrections, we can always decompose the gluon fusion cross section in terms of the Yukawa couplings Y_i :

$$\sigma_{ggH} = \sum_{i \leq j} Y_i Y_j \sigma_{ij}. \quad (4.14)$$

We call

$$\sigma_{i \times j} = Y_i Y_j \sigma_{ij}, \quad (4.15)$$

the *i-j-interference contribution* and

$$\sigma_i = Y_i^2 \sigma_{ii} \quad (4.16)$$

the *pure-i contribution* to the cross section. Both contributions are depicted at LO in Fig. 4.3. Clearly, the dominant contribution for the lighter quark flavors comes from the interference with

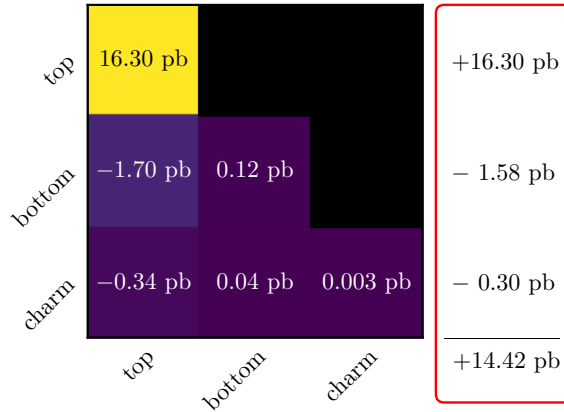


Figure 4.3: σ_i (diagonals) and $\sigma_{i \times j}$ (off-diagonals) at LO for the three heaviest quark flavors. The red box indicates the sum of each row, and hence the combined effects of each additional flavor. Computational setup is described in the conventions

the top-quark. The pure-bottom contribution is already below a percent and the pure-charm quark mass effects are completely negligible. The inclusion of the charm quark lowers the total cross section by around 2%, making it relevant for high precision predictions.

² Values of masses and coupling constants are provided in the conventions.

4.3 THE HEAVY-TOP LIMIT

The computation of the Higgs production cross section in full QCD is quite challenging. As we saw above, even at leading order we encounter loop integrals with two mass scales. It is therefore maybe not surprising that the first NLO corrections to this process were actually computed in an approximation framework [30]. In the approximation, we assume that the quark, which is coupling to the Higgs is infinitely heavy. That means we are only interested in the leading term of the LME.

The finite distance interaction of the gluon and the Higgs will therefore shrink down to a point like vertex, which we can describe with the effective Lagrangian

$$\mathcal{L}_{\text{HTL}}^{(0)} = \mathcal{L}_{\text{QCD}}^{(n_f-1)} + \frac{\alpha_s}{\pi} C^{(0)} \frac{H}{v} \frac{1}{4} G_{\mu\nu}^a G^{a\mu\nu}. \quad (4.17)$$

We see that the coupling constant now has mass dimension -1 , so the theory will not be UV renormalizable. That means that we cannot absorb all UV divergences into multiplicative renormalization constants as we did for the SM (see Eq. (2.31)), but we will generate more and more independent terms in our Lagrangian to cancel all appearing divergences. On the other hand, as long as we restrict ourselves to QCD corrections, and hence only single operator insertions, we can treat the color singlet Higgs as a constant, and renormalize only the gauge invariant operator

$$\mathcal{O}_1 \equiv -1/4 G_{\mu\nu}^a G^{a\mu\nu}. \quad (4.18)$$

To indicate the perturbative order we gave the Lagrangian in Eq. (4.17) a superscript. The superscript $n_f - 1$ of the QCD Lagrangian specifies the number of active flavors. It was reduced by one, since the heaviest quark flavor was integrated out. The constant $C^{(0)}$ is called a *Wilson coefficient*, and it needs to be matched to the full theory in the infinite quark mass limit. At LO for example, we find that the Higgs-gluon form factor in the effective theory simply reads

$$\mathcal{C}^{(0)} = C^{(0)}. \quad (4.19)$$

If we compare this to the leading term of our LME (4.8), we find

$$C^{(0)} = \frac{2}{3} T_F. \quad (4.20)$$

The main benefit of the approximation lies in the reduced complexity. By integrating out the top quark, we have reduced a loop-induced process to a tree-level process. Moreover, the top-quark mass is eliminated as a scale, hence the appearing Feynman integrals will generally be much simpler to solve.

Beyond LO gauge invariant operator like \mathcal{O}_1 can mix under renormalization with other gauge invariant operators but notably also with operators which are not gauge invariant. In general, we distinguish two types of operators: *Type-II operators*, which give zero when sandwiched between physical states, and *type-I operators*, which can give non-zero matrix elements. The type-II operators can be further subcategorized into operators vanishing by the equation of motion (*type-II_a operators*), and all other operators (*type-II_b operators*). For a polynomial operator with ghost number zero satisfying

$$s\mathcal{O} = 0, \quad (4.21)$$

where s is the *linearized Slavnov operator*, one can proof [31, 32, 33] that

$$\mathcal{O} = sF + \text{gauge invariant operators}. \quad (4.22)$$

Operators of the form sF are also called *Bechi-Rouet-Stora-Tyutin-* (BRST-) *exact operators*, and they vanish between physical states. For \mathcal{O}_1 the above conditions are met, allowing us to conclude that the \mathcal{O}_{II} operators are BRST-exact. This can be leveraged to find the complete operator basis:

$$\begin{aligned} \mathcal{O}_I & \left\{ \begin{array}{l} \mathcal{O}_1 = -\frac{1}{4}G_{\mu\nu}^a G^{a\mu\nu}, \\ \mathcal{O}_2 = m_q \bar{q}q, \end{array} \right. \\ \mathcal{O}_{II_a} & \left\{ \begin{array}{l} \mathcal{O}_3 = \bar{q} \left(\frac{i}{2} \overleftrightarrow{D} - m \right) q, \end{array} \right. \\ \mathcal{O}_{II_b} & \left\{ \begin{array}{l} \mathcal{O}_4 = A^{a\mu} D^\nu F_{\nu\mu}^a + g \bar{q} \not{A} q - \partial^\mu \bar{c}^a \partial_\mu c^a, \\ \mathcal{O}_5 = D_\mu \partial^\mu \bar{c}^a c^a. \end{array} \right. \end{aligned} \quad (4.23)$$

Since operators of type II cannot generate non-vanishing S -matrix elements through renormalization the renormalization matrix must have the general structure

$$\begin{pmatrix} \mathcal{O}_I^R \\ \mathcal{O}_{II}^R \end{pmatrix} = \begin{pmatrix} z^{I,I} & z^{I,II} \\ 0 & z^{II,II} \end{pmatrix} \begin{pmatrix} \mathcal{O}_I^B \\ \mathcal{O}_{II}^B \end{pmatrix}. \quad (4.24)$$

The final form of our effective Lagrangian therefore reads

$$\mathcal{L}_{\text{HTL}} = \mathcal{L}_{\text{QCD}}^{(5)} + \frac{\alpha_s}{\pi} \frac{H}{v} \sum_i C_i^B \mathcal{O}_i^B. \quad (4.25)$$

As usual, we replace the bare quantities by their renormalized counter parts

$$C_i^B \mathcal{O}_i^B = C_i^B Z_{ij}^{-1} \mathcal{O}_j^R, \quad (4.26)$$

and we identify

$$C^R = (Z^{-1})^T C^B. \quad (4.27)$$

Using the RGE we find that the *anomalous dimension* matrix of the Wilson coefficients is determined through

$$\frac{dC^R}{d \ln \mu} = \left(Z \frac{d(Z^{-1})}{d \ln \mu} \right)^T C^R = - \left(\frac{dZ}{d \ln \mu} Z^{-1} \right)^T \equiv \gamma^T C^R. \quad (4.28)$$

With the structure of the renormalization matrix (4.24), we arrive at an important conclusion: The Wilson coefficients of type-II operators cannot mix into the Wilson coefficients of type-I operators through the running in the scale. Since the type-II operators render no contribution to the scattering matrix element, we can focus our attention on the gauge invariant operators and their Wilson coefficients.

We now want to determine the I, I part of the renormalization matrix, i.e. $z^{I,I}$ to determine the running of the Wilson coefficients. Let us start by defining the generating functional

$$\begin{aligned} Z[J] & \equiv z[J]/z[0], \quad z[J] \equiv \int \prod_i \mathcal{D}\Phi_j e^{i(S+J \cdot \Phi)}, \quad S = S[A, c, \bar{c}, q, \bar{q}] \equiv \int d^d x \mathcal{L}, \\ J & = (J^\mu, \bar{J}, J, \bar{\eta}, \eta), \quad \Phi = \left(\frac{1}{g} A_\mu, c, \bar{c}, q, \bar{q} \right), \end{aligned} \quad (4.29)$$

with the Lagrangian

$$\mathcal{L} \equiv -\frac{1}{4g^2} F_{\mu\nu}^a F^{a\mu\nu} - \frac{1}{2\xi g^2} (\partial \cdot A)^2 + \partial^\mu \bar{c}^a D_\mu c^a + \bar{q} \left(\frac{i \overleftrightarrow{D}}{2} - m_q \right) q. \quad (4.30)$$

The Lagrangian is the QCD Lagrangian with only one active quark flavor and rescaled gauge fields

$$A_\mu^a \longrightarrow \frac{1}{g} A_\mu^a. \quad (4.31)$$

The operators in Eq. (4.23) can now be generated by applying the differential operators³

$$\begin{aligned} D_1 &= -\frac{1}{2}g \frac{\partial}{\partial g} + \xi \frac{\partial}{\partial \xi} - \frac{1}{2}J_\mu \cdot \frac{\delta}{\delta J_\mu}, \\ D_2 &= -m_q \frac{\partial}{\partial m_q}, \end{aligned} \quad (4.32)$$

on the generating functional

$$z_{\mathcal{O}_k}[J] \equiv \int \prod_j \mathcal{D}\Phi_j \hat{\mathcal{O}}_k(0) e^{i(S+J\cdot\Phi)} = -iD_k z[J]. \quad (4.33)$$

Here $\hat{\mathcal{O}}_k(0)$ is the Fourier transform of the operator $\mathcal{O}(x)$ at zero momentum. The normalization of the generating functional then properly subtracts the vacuum expectation value of the operators

$$-iD_k Z[J] = \frac{1}{z[0]} \int \prod_j \mathcal{D}\Phi_j \left(\hat{\mathcal{O}}_k(0) - \langle \Omega | \mathcal{O}_k(0) | \Omega \rangle \right) e^{i(S+J\cdot\Phi)} \equiv Z_{\mathcal{O}_k}. \quad (4.34)$$

In the $\overline{\text{MS}}$ scheme, the R -operation commutes with the differential operators in Eq. (4.32), i.e. the renormalized operators can be generated from the renormalized generating functional

$$Z_{\mathcal{O}_k^R} = -iD_k Z^R[J], \quad (4.35)$$

where the renormalized generating functional is defined as

$$\begin{aligned} Z^R[J] &= z^R[J]/z^R[0], \\ z^R[J] &= \int \prod_i \mathcal{D}\Phi_i e^{i(S^R+J\cdot\Phi)}, \\ S^R &\equiv S[Z_3'^{1/2} A^R, Z_3'^{-1/2} c^R, \tilde{Z}_3'^{-1/2} \bar{c}^R, Z_2'^{1/2} q^R, Z_2'^{1/2} \bar{q}^R, Z_g g, Z_m m_q, Z_g^{-2} Z_3' \xi^R]. \end{aligned} \quad (4.36)$$

Using the chain rule we find that

$$-iD_k z^R[J] = \int \prod_j \mathcal{D}\Phi_j \left[\hat{\mathcal{O}}_k(0) + \sum_i (D_k \ln Z_i) \frac{\partial S^R}{\partial \ln Z_i} \right] e^{iS^R+J\cdot\Phi}, \quad Z_i \in \{Z_3', \tilde{Z}_3', Z_2, Z_g, Z_m\}. \quad (4.37)$$

And with

$$Z_g \frac{\partial S^R}{\partial Z_g} = -2\hat{\mathcal{O}}_1(0), \quad \text{and} \quad Z_m \frac{\partial S^R}{\partial Z_m} = -\hat{\mathcal{O}}_2(0), \quad (4.38)$$

³ We only provide the operators for the type-I operators, since they are the only ones necessary for computing physical amplitudes.

we find that the renormalization constants are given by

$$\begin{aligned} z_{11}^{I,I} &= 1 - 2D_1 \ln Z_g = 1 + g \frac{\partial \ln Z_g}{\partial g}, & z_{12}^{I,I} &= -D_1 \ln Z_m = \frac{g}{2} \frac{\partial \ln Z_m}{\partial g} \\ z_{21}^{I,I} &= 0, & z_{22}^{I,I} &= 1. \end{aligned} \quad (4.39)$$

Here we made use of the fact, that the $\overline{\text{MS}}$ -renormalization constants are independent of the quark mass and the gauge parameter. We can rewrite the appearing derivatives in terms of the β -function and the mass-anomalous dimension. Indeed,

$$\begin{aligned} \frac{4\pi}{\alpha_s} \bar{\beta} &\equiv \frac{d \ln \alpha_s}{d \ln \mu} = -\frac{d \ln Z_{\alpha_s}}{d \ln \mu} = -\left(\frac{\partial \ln Z_{\alpha_s}}{\partial \ln \alpha_s} \frac{d \ln \alpha_s}{d \ln \mu} + \frac{\partial \ln Z_{\alpha_s}}{\partial \ln \mu} \right) = -\left(\frac{\bar{\beta}}{\alpha_s} \frac{\partial \ln Z_{\alpha_s}}{\partial \ln \alpha_s} + 2\epsilon \right) \\ &\Rightarrow \frac{\partial \ln Z_{\alpha_s}}{\partial \ln \alpha_s} = g \frac{\partial \ln Z_g}{\partial g} = -4\pi - 2\epsilon \frac{\alpha_s}{\bar{\beta}} = -1 + \frac{1}{1 - \frac{\beta}{2\epsilon} \frac{4\pi}{\alpha_s}}, \end{aligned} \quad (4.40)$$

where in the last step we used the relation between the d - and four-dimensional β -functions

$$\bar{\beta} = \beta - 2\epsilon \frac{\alpha_s}{4\pi}. \quad (4.41)$$

Similarly, we find

$$\begin{aligned} \gamma_m &\equiv -\frac{d \ln m_q}{d \ln \mu} = \frac{d \ln Z_m}{d \ln \mu} = \frac{\partial \ln Z_m}{\partial \ln \alpha_s} \frac{\partial \ln \alpha_s}{\partial \ln \mu} = \frac{\partial \ln Z_m}{\partial \ln \alpha_s} \frac{4\pi}{\alpha_s} \bar{\beta} \\ &\Rightarrow \frac{\partial \ln Z_m}{\partial \ln \alpha_s} = g \frac{\partial \ln Z_m}{\partial g} = \frac{\alpha_s}{4\pi} \frac{1}{\bar{\beta}} \gamma_m = -\frac{\gamma_m}{2\epsilon} \frac{1}{1 - \frac{\beta}{2\epsilon} \frac{4\pi}{\alpha_s}} \end{aligned} \quad (4.42)$$

Finally, we want to use the above results to calculate the anomalous dimension matrix in Eq. (4.28). The entries of the renormalization constant only depend on scale through the coupling constant, i.e.

$$\gamma^{I,I} = -\frac{dz^{I,I}}{d \ln \mu} (z^{I,I})^{-1} \Big|_{\epsilon=0} = -\frac{\partial z^{I,I}}{\partial \alpha_s} (z^{I,I})^{-1} 4\pi \bar{\beta} \Big|_{\epsilon=0} = \frac{\partial z^{I,I(1)}}{\partial \alpha_s} 2\alpha_s. \quad (4.43)$$

Where we used that $z^{I,I}$ consists only of poles in the $\overline{\text{MS}}$ scheme, and once again applied the relation between the β -functions in Eq. (4.41). $z^{I,I(1)}$ denotes the residue of the renormalization matrix

$$z^{I,I} = \mathbb{1} + \sum_{i=1} z^{I,I(i)} \epsilon^{-i}. \quad (4.44)$$

We then find for the anomalous dimension matrix

$$\gamma^{I,I} = \begin{pmatrix} 4\pi\alpha_s \frac{d}{d\alpha_s} \left(\frac{\beta}{\alpha_s} \right) & -\alpha_s \frac{d\gamma_m}{d\alpha_s} \\ 0 & 0 \end{pmatrix}. \quad (4.45)$$

The structure of this matrix reveals, that the C_1 Wilson coefficient, which is relevant coefficient for the HTL, is completely independent of the other Wilson coefficients. The RGE for the Wilson coefficient (4.28) can now be written as

$$\frac{\partial C_1}{\partial \alpha_s} 4\pi\beta + \frac{\partial C_1}{\partial \ln \mu} = 4\pi\alpha_s \frac{d}{d\alpha_s} \left(\frac{\beta}{\alpha_s} \right). \quad (4.46)$$

The *beta*-function has the general expansion

$$\beta = \left(\frac{\alpha_s}{4\pi}\right)^2 \sum_{i=0} \beta_i \left(\frac{\alpha_s}{4\pi}\right)^i. \quad (4.47)$$

For example at one-, and two-loop, it can be shown [34, 35, 36, 37, 38, 39]

$$\begin{aligned} \beta_0 &= \frac{11}{3}C_A - \frac{4}{3}T_F n_f, \\ \beta_1 &= \frac{34}{3}C_A^2 - \frac{20}{3}C_A T_F n_f - 4C_F T_F n_f. \end{aligned} \quad (4.48)$$

We can solve the partial differential equation in Eq. (4.46) perturbatively by proposing the Ansatz

$$\begin{aligned} C_1 &= C_1^{(0,0)} + \frac{\alpha_s}{4\pi} \left(C_1^{(1,0)} + C_1^{(1,1)} \ln \frac{\mu}{\mu_0} \right) \\ &+ \left(\frac{\alpha_s}{4\pi} \right)^2 \left(C_1^{(2,0)} + C_1^{(2,1)} \ln \frac{\mu}{\mu_0} + C_1^{(2,2)} \ln^2 \frac{\mu}{\mu_0} \right) + \mathcal{O}(\alpha_s^3). \end{aligned} \quad (4.49)$$

The constants coefficients $C_1^{(i,0)}$ mark the initial conditions; they need to be matched to the full theory in the infinite mass limit. The coefficients of the logarithms on the other hand can be determined through a comparison of coefficients, they read

$$C_1^{(1,1)} = 0, \quad C_1^{(2,1)} = C_1^{(0,0)}\beta_1 - C_1^{(1,0)}\beta_0, \quad C_1^{(2,2)} = 0. \quad (4.50)$$

It is clear from the structure of the differential equation, that the all coefficients $C_1^{(i,i)}$ are in fact all zero except for $C_1^{(0,0)}$.

By expanding the Higgs-gluon form for large quark masses we were able to determine the LO Wilson coefficient⁴. Of course, if we would need the full Higgs-gluon form factor to determine the Wilson coefficient, the HTL would be of little use, since it would not bring any simplifications. Fortunately, the large quark mass limit can already be used at the integrand level using the large mass expansion,

4.4 HIGHER-ORDER CORRECTIONS

Here I outline how to perform higher order corrections.

4.5 THEORY STATUS

Here I describe what is already known about the gluon-gluon fusion channel. I explain the theory uncertainties.

⁴ Notice the different signs in Eqs. (4.17) and (4.25). So the Wilson coefficients are related by $C_1^{(0,0)} = -C^{(0)} = -\frac{2}{3}T_F$.

5 | COMPUTATIONAL DETAILS

Description of this chapter.

5.1 COMPUTING THE AMPLITUDES

Here I

5.1.1 The Real-Real Corrections

5.1.2 The Real-Virtual Corrections

5.1.3 The Virtual-Virtual Corrections

5.2 $\overline{\text{MS}}$ -SCHEME

5.3 THE 4-FLAVOUR SCHEME

5.4 PERFORMING THE PHASE-SPACE INTEGRATION

6 | RESULTS AND DISCUSSION

Description of this chapter.

6.1 TOTAL CROSS SECTION

6.1.1 Effects of Finite Top-Quark Masses

6.1.2 Effects of Finite Bottom-Quark Masses

6.2 DIFFERENTIAL CROSS SECTION

7 | CONCLUSIONS

Here are my conclusions.

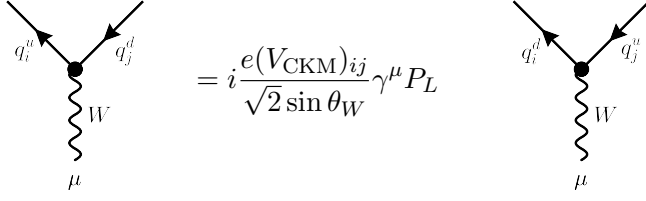
In this chapter we list all Feynman rules of the SM. We choose to work in a unitary gauge, meaning that the all Goldstone-bosons decouple and there are no unphysical particles in the electroweak sector. In the QCD sector, we work in the R_ξ gauge, i.e. we have unphysical particles in the form of *Faddeev-Popov ghosts*. If not otherwise specified, the momenta on every line are defined as incoming.

Propagators:

$$\begin{aligned}
 a, \mu \quad \text{---} \overline{\text{---}} \overline{\text{---}} \overline{\text{---}} \overline{\text{---}} \overline{\text{---}} \overline{\text{---}} \overline{\text{---}} \overline{\text{---}} \overline{\text{---}} \overline{\text{---}} \text{---} \quad b, \nu &= i \frac{\delta^{ab}}{k^2 + i0^+} \left[-g_{\mu\nu} + (1 - \xi) \frac{k_\mu k_\nu}{k^2 + i0^+} \right] \\
 i \quad \text{---} \overline{\text{---}} \overline{\text{---}} \overline{\text{---}} \overline{\text{---}} \overline{\text{---}} \overline{\text{---}} \overline{\text{---}} \overline{\text{---}} \overline{\text{---}} \text{---} \quad j &= i \delta_{ij} \frac{\not{k} + m}{k^2 - m^2 + i0^+} \\
 \text{---} \overline{\text{---}} \overline{\text{---}} \overline{\text{---}} \overline{\text{---}} \overline{\text{---}} \overline{\text{---}} \overline{\text{---}} \overline{\text{---}} \overline{\text{---}} \text{---} &= i \frac{1}{k^2 - m_H^2 + i0^+} \\
 \mu \quad \text{---} \overline{\text{---}} \overline{\text{---}} \overline{\text{---}} \overline{\text{---}} \overline{\text{---}} \overline{\text{---}} \overline{\text{---}} \overline{\text{---}} \overline{\text{---}} \text{---} \quad \nu &= i \frac{-g_{\mu\nu}}{k^2 + i0^+} \\
 \mu \quad \text{---} \overline{\text{---}} \overline{\text{---}} \overline{\text{---}} \overline{\text{---}} \overline{\text{---}} \overline{\text{---}} \overline{\text{---}} \overline{\text{---}} \overline{\text{---}} \text{---} \quad \nu &= i \frac{1}{k^2 - m_W^2 + i0^+} \left(-g_{\mu\nu} + \frac{k_\mu k_\nu}{m_W^2 + i0^+} \right) \\
 \mu \quad \text{---} \overline{\text{---}} \overline{\text{---}} \overline{\text{---}} \overline{\text{---}} \overline{\text{---}} \overline{\text{---}} \overline{\text{---}} \overline{\text{---}} \overline{\text{---}} \text{---} \quad \nu &= i \frac{1}{k^2 - m_Z^2 + i0^+} \left(-g_{\mu\nu} + \frac{k_\mu k_\nu}{m_Z^2 + i0^+} \right) \\
 a \quad \text{---} \overline{\text{---}} \overline{\text{---}} \overline{\text{---}} \overline{\text{---}} \overline{\text{---}} \overline{\text{---}} \overline{\text{---}} \overline{\text{---}} \overline{\text{---}} \text{---} \quad b &= i \frac{\delta^{ab}}{k^2 + i0^+}
 \end{aligned}$$

Fermion–Gauge-Boson Vertices:

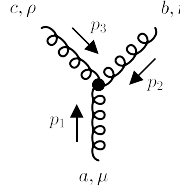
$$\begin{aligned}
 \begin{array}{c} i \\ \swarrow \\ \bullet \\ \searrow \\ j \\ \downarrow \\ \text{---} \overline{\text{---}} \overline{\text{---}} \overline{\text{---}} \overline{\text{---}} \overline{\text{---}} \overline{\text{---}} \overline{\text{---}} \overline{\text{---}} \text{---} \\ a, \mu \end{array} &= ig \gamma^\mu T_{ij}^a \\
 \begin{array}{c} \swarrow \\ \bullet \\ \searrow \\ \downarrow \\ \text{---} \overline{\text{---}} \overline{\text{---}} \overline{\text{---}} \overline{\text{---}} \overline{\text{---}} \overline{\text{---}} \overline{\text{---}} \overline{\text{---}} \text{---} \\ \mu \end{array} &= -ie \gamma^\mu Q \\
 \begin{array}{c} a \\ \swarrow \\ \bullet \\ \searrow \\ b \\ \downarrow \\ \text{---} \overline{\text{---}} \overline{\text{---}} \overline{\text{---}} \overline{\text{---}} \overline{\text{---}} \overline{\text{---}} \overline{\text{---}} \overline{\text{---}} \text{---} \\ c, \mu \end{array} &= g f^{abc} p^\mu \\
 \begin{array}{c} \swarrow \\ \bullet \\ \searrow \\ \downarrow \\ \text{---} \overline{\text{---}} \overline{\text{---}} \overline{\text{---}} \overline{\text{---}} \overline{\text{---}} \overline{\text{---}} \overline{\text{---}} \overline{\text{---}} \text{---} \\ \mu \end{array} &= i \frac{e}{\sin \theta_W \cos \theta_W} \gamma^\mu \\
 &\quad \times (I^3 P_L - Q \sin^2 \theta_W)
 \end{aligned}$$



Two Feynman diagrams showing the coupling of a W boson to fermions. The left diagram shows a quark line with incoming momentum q_i^u and outgoing momentum q_j^d , and a W boson line with index μ . The right diagram shows a lepton line with incoming momentum q_i^l and outgoing momentum q_j^u , and a W boson line with index μ .

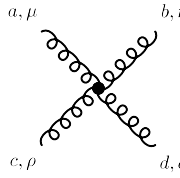
$$= i \frac{e(V_{\text{CKM}})_{ij}}{\sqrt{2} \sin \theta_W} \gamma^\mu P_L \quad = i \frac{e(V_{\text{CKM}})_{ji}^*}{\sqrt{2} \sin \theta_W} \gamma^\mu P_L$$

Gauge-Boson Self Interactions:



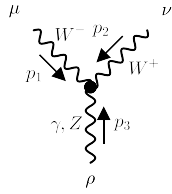
Feynman diagram for the three-gluon vertex. Three gluon lines meet at a central vertex. The incoming lines are labeled c, ρ and b, ν with momenta p_1 and p_2 respectively. The outgoing line is labeled a, μ with momentum p_3 .

$$= g f^{abc} ((p_1^\rho - p_2^\rho) g^{\mu\nu} + (p_2^\mu - p_3^\mu) g^{\nu\rho} + (p_3^\nu - p_1^\nu) g^{\rho\mu})$$



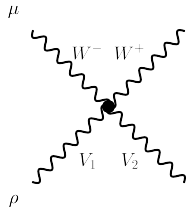
Feynman diagram for the four-gluon vertex. Four gluon lines meet at a central vertex. The incoming lines are labeled a, μ and c, ρ with momenta p_1 and p_2 respectively. The outgoing lines are labeled b, ν and d, σ with momenta p_3 and p_4 respectively.

$$= -ig^2 (f^{abe} f^{cde} (g^{\mu\rho} g^{\nu\sigma} - g^{\mu\sigma} g^{\nu\rho}) + f^{ace} f^{bde} (g^{\mu\nu} g^{\rho\sigma} - g^{\mu\sigma} g^{\nu\rho}) + f^{ade} f^{bce} (g^{\mu\nu} g^{\rho\sigma} - g^{\mu\rho} g^{\nu\sigma}))$$



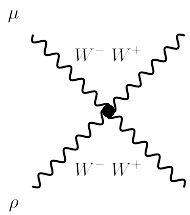
Feynman diagram for the WWV vertex. Two W boson lines (labeled W^- and W^+) and a photon/Z boson line (labeled γ, Z) meet at a central vertex. The incoming lines are labeled μ and ν with momenta p_1 and p_2 respectively. The outgoing line is labeled ρ with momentum p_3 .

$$= i \frac{e}{\sin \theta_W} ((p_1^\rho - p_2^\rho) g^{\mu\nu} + (p_2^\mu - p_3^\mu) g^{\nu\rho} + (p_3^\nu - p_1^\nu) g^{\rho\mu}) \times \begin{cases} -\sin \theta_W & \text{for } \gamma \\ \cos \theta_W & \text{for } Z \end{cases}$$



Feynman diagram for the WWV^2 vertex. Two W boson lines (labeled W^- and W^+) and two photon/Z boson lines (labeled V_1 and V_2) meet at a central vertex. The incoming lines are labeled μ and ν with momenta p_1 and p_2 respectively. The outgoing lines are labeled ρ and σ with momenta p_3 and p_4 respectively.

$$= i \frac{e^2}{\sin^2 \theta_W} (g^{\mu\sigma} g^{\nu\rho} + g^{\mu\rho} g^{\nu\sigma} - 2g^{\mu\nu} g^{\rho\sigma}) \times \prod_{i=1}^2 \begin{cases} -\sin \theta_W & \text{if } V_i = \gamma \\ \cos \theta_W & \text{if } V_i = Z \end{cases}$$



Feynman diagram for the WWV^2 vertex (crossed). Two W boson lines (labeled W^- and W^+) and two photon/Z boson lines (labeled W^- and W^+) meet at a central vertex. The incoming lines are labeled μ and ν with momenta p_1 and p_2 respectively. The outgoing lines are labeled ρ and σ with momenta p_3 and p_4 respectively.

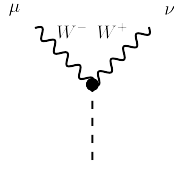
$$= i \frac{e^2}{\sin^2 \theta_W} (2g^{\mu\rho} g^{\nu\sigma} - g^{\mu\nu} g^{\rho\sigma} - g^{\mu\sigma} g^{\nu\rho})$$

Higgs Interactions:

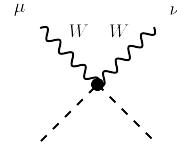


Two Feynman diagrams showing Higgs interactions. The left diagram shows a fermion line with incoming momentum i and outgoing momentum j , and a Higgs boson line (dashed) with index μ . The right diagram shows a Higgs boson line (dashed) with index μ and a Higgs boson line (dashed) with index ν .

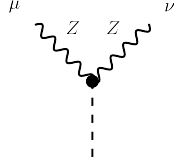
$$= -i \frac{m_q}{v} \delta_{ij} \quad = -i \frac{3m_H^2}{v}$$



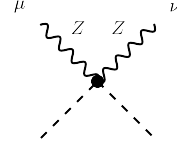
$$= i \frac{e}{\sin \theta_W} m_W g^{\mu\nu}$$



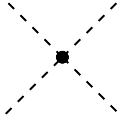
$$= i \frac{e^2}{2 \sin^2 \theta_W} g^{\mu\nu}$$



$$= i \frac{e}{\sin \theta_W \cos \theta_W} m_Z g^{\mu\nu}$$



$$= i \frac{e^2}{2 \sin^2 \theta_W \cos^2 \theta_W} g^{\mu\nu}$$



$$= -i \frac{3m_H^2}{v^2} g^{\mu\nu}$$

BIBLIOGRAPHY

- [1] Michał Czakon, Felix Schlenker, and Tom Schellenberger. “Revisiting the double-soft asymptotics of one-loop amplitudes in massless QCD.” In: *JHEP* 04 (2023), p. 065. DOI: [10.1007/JHEP04\(2023\)065](https://doi.org/10.1007/JHEP04(2023)065). arXiv: [2211.06465](https://arxiv.org/abs/2211.06465) [hep-ph].
- [2] Michał Czakon, Felix Schlenker, and Tom Schellenberger. “Subleading effects in soft-gluon emission at one-loop in massless QCD.” In: *JHEP* 12 (2023), p. 126. DOI: [10.1007/JHEP12\(2023\)126](https://doi.org/10.1007/JHEP12(2023)126). arXiv: [2307.02286](https://arxiv.org/abs/2307.02286) [hep-ph].
- [3] Michał Czakon et al. “Top-Bottom Interference Contribution to Fully Inclusive Higgs Production.” In: *Phys. Rev. Lett.* 132.21 (2024), p. 211902. DOI: [10.1103/PhysRevLett.132.211902](https://doi.org/10.1103/PhysRevLett.132.211902). arXiv: [2312.09896](https://arxiv.org/abs/2312.09896) [hep-ph].
- [4] Michał Czakon et al. “Quark mass effects in Higgs production.” In: *JHEP* 10 (2024), p. 210. DOI: [10.1007/JHEP10\(2024\)210](https://doi.org/10.1007/JHEP10(2024)210). arXiv: [2407.12413](https://arxiv.org/abs/2407.12413) [hep-ph].
- [5] Izaak Neutelings. *Izaak neutelings*. Mar. 2024. URL: https://tikz.net/sm_particles/.
- [6] Stefan Weinzierl. *Feynman Integrals. A Comprehensive Treatment for Students and Researchers*. UNITEXT for Physics. Springer, 2022. ISBN: 978-3-030-99557-7, 978-3-030-99560-7, 978-3-030-99558-4. DOI: [10.1007/978-3-030-99558-4](https://doi.org/10.1007/978-3-030-99558-4). arXiv: [2201.03593](https://arxiv.org/abs/2201.03593) [hep-th].
- [7] Gerard 't Hooft. “Renormalizable Lagrangians for Massive Yang-Mills Fields.” In: *Nucl. Phys. B* 35 (1971). Ed. by J. C. Taylor, pp. 167–188. DOI: [10.1016/0550-3213\(71\)90139-8](https://doi.org/10.1016/0550-3213(71)90139-8).
- [8] Gerard 't Hooft and M. J. G. Veltman. “Regularization and Renormalization of Gauge Fields.” In: *Nucl. Phys. B* 44 (1972), pp. 189–213. DOI: [10.1016/0550-3213\(72\)90279-9](https://doi.org/10.1016/0550-3213(72)90279-9).
- [9] Andy Buckley et al. “LHAPDF6: parton density access in the LHC precision era.” In: *Eur. Phys. J. C* 75 (2015), p. 132. DOI: [10.1140/epjc/s10052-015-3318-8](https://doi.org/10.1140/epjc/s10052-015-3318-8). arXiv: [1412.7420](https://arxiv.org/abs/1412.7420) [hep-ph].
- [10] Richard D. Ball et al. “Parton distributions from high-precision collider data.” In: *Eur. Phys. J. C* 77.10 (2017), p. 663. DOI: [10.1140/epjc/s10052-017-5199-5](https://doi.org/10.1140/epjc/s10052-017-5199-5). arXiv: [1706.00428](https://arxiv.org/abs/1706.00428) [hep-ph].
- [11] John C. Collins, Davison E. Soper, and George F. Sterman. “Factorization of Hard Processes in QCD.” In: *Adv. Ser. Direct. High Energy Phys.* 5 (1989), pp. 1–91. DOI: [10.1142/9789814503266_0001](https://doi.org/10.1142/9789814503266_0001). arXiv: [hep-ph/0409313](https://arxiv.org/abs/hep-ph/0409313).
- [12] Yuri L. Dokshitzer. “Calculation of the Structure Functions for Deep Inelastic Scattering and e^+e^- Annihilation by Perturbation Theory in Quantum Chromodynamics.” In: *Sov. Phys. JETP* 46 (1977), pp. 641–653.
- [13] V. N. Gribov and L. N. Lipatov. “Deep inelastic $e p$ scattering in perturbation theory.” In: *Sov. J. Nucl. Phys.* 15 (1972), pp. 438–450.
- [14] Guido Altarelli and G. Parisi. “Asymptotic Freedom in Parton Language.” In: *Nucl. Phys. B* 126 (1977), pp. 298–318. DOI: [10.1016/0550-3213\(77\)90384-4](https://doi.org/10.1016/0550-3213(77)90384-4).
- [15] T. Kinoshita and A. Ukawa. “Mass Singularities of Feynman Amplitudes.” In: *Lect. Notes Phys.* 39 (1975). Ed. by Huzihiro Araki, pp. 55–58. DOI: [10.1007/BFb0013300](https://doi.org/10.1007/BFb0013300).

- [16] T. D. Lee and M. Nauenberg. “Degenerate Systems and Mass Singularities.” In: *Phys. Rev.* 133 (1964). Ed. by G. Feinberg, B1549–B1562. DOI: [10.1103/PhysRev.133.B1549](#).
- [17] Charalampos Anastasiou and Kirill Melnikov. “Higgs boson production at hadron colliders in NNLO QCD.” In: *Nucl. Phys. B* 646 (2002), pp. 220–256. DOI: [10.1016/S0550-3213\(02\)00837-4](#). arXiv: [hep-ph/0207004](#).
- [18] Falko Dulat et al. “Higgs-differential cross section at NNLO in dimensional regularisation.” In: *JHEP* 07 (2017), p. 017. DOI: [10.1007/JHEP07\(2017\)017](#). arXiv: [1704.08220 \[hep-ph\]](#).
- [19] Markus A. Ebert, Bernhard Mistlberger, and Gherardo Vita. “ N -jettiness beam functions at N³LO.” In: *JHEP* 09 (2020), p. 143. DOI: [10.1007/JHEP09\(2020\)143](#). arXiv: [2006.03056 \[hep-ph\]](#).
- [20] Daniel Baranowski et al. “Zero-jettiness soft function to third order in perturbative QCD.” In: (Sept. 2024). arXiv: [2409.11042 \[hep-ph\]](#).
- [21] Daniel Baranowski et al. “Triple real-emission contribution to the zero-jettiness soft function at N³LO in QCD.” In: (Dec. 2024). arXiv: [2412.14001 \[hep-ph\]](#).
- [22] John M. Campbell et al. “The NNLO QCD soft function for 1-jettiness.” In: *Eur. Phys. J. C* 78.3 (2018), p. 234. DOI: [10.1140/epjc/s10052-018-5732-1](#). arXiv: [1711.09984 \[hep-ph\]](#).
- [23] Thomas Becher and Guido Bell. “The gluon jet function at two-loop order.” In: *Phys. Lett. B* 695 (2011), pp. 252–258. DOI: [10.1016/j.physletb.2010.11.036](#). arXiv: [1008.1936 \[hep-ph\]](#).
- [24] Thomas Becher and Matthias Neubert. “Toward a NNLO calculation of the anti- $B \rightarrow X(s)$ gamma decay rate with a cut on photon energy. II. Two-loop result for the jet function.” In: *Phys. Lett. B* 637 (2006), pp. 251–259. DOI: [10.1016/j.physletb.2006.04.046](#). arXiv: [hep-ph/0603140](#).
- [25] Radja Boughezal, Xiaohui Liu, and Frank Petriello. “ N -jettiness soft function at next-to-next-to-leading order.” In: *Phys. Rev. D* 91.9 (2015), p. 094035. DOI: [10.1103/PhysRevD.91.094035](#). arXiv: [1504.02540 \[hep-ph\]](#).
- [26] Michał Czakon et al. “Single-jet inclusive rates with exact color at $\mathcal{O}(\alpha_s^4)$.” In: *JHEP* 10 (2019), p. 262. DOI: [10.1007/JHEP10\(2019\)262](#). arXiv: [1907.12911 \[hep-ph\]](#).
- [27] M. Czakon. “A novel subtraction scheme for double-real radiation at NNLO.” In: *Phys. Lett. B* 693 (2010), pp. 259–268. DOI: [10.1016/j.physletb.2010.08.036](#). arXiv: [1005.0274 \[hep-ph\]](#).
- [28] H. M. Georgi et al. “Higgs Bosons from Two Gluon Annihilation in Proton Proton Collisions.” In: *Phys. Rev. Lett.* 40 (1978), p. 692. DOI: [10.1103/PhysRevLett.40.692](#).
- [29] Michał L. Czakon and Marco Niggetiedt. “Exact quark-mass dependence of the Higgs-gluon form factor at three loops in QCD.” In: *JHEP* 05 (2020), p. 149. DOI: [10.1007/JHEP05\(2020\)149](#). arXiv: [2001.03008 \[hep-ph\]](#).
- [30] S. Dawson. “Radiative corrections to Higgs boson production.” In: *Nucl. Phys. B* 359 (1991), pp. 283–300. DOI: [10.1016/0550-3213\(91\)90061-2](#).
- [31] H. Kluberg-Stern and J. B. Zuber. “Ward Identities and Some Clues to the Renormalization of Gauge Invariant Operators.” In: *Phys. Rev. D* 12 (1975), pp. 467–481. DOI: [10.1103/PhysRevD.12.467](#).

- [32] Satish D. Joglekar and Benjamin W. Lee. “General Theory of Renormalization of Gauge Invariant Operators.” In: *Annals Phys.* 97 (1976), p. 160. DOI: [10.1016/0003-4916\(76\)90225-6](#).
- [33] Marc Henneaux, Axel Kleinschmidt, and Gustavo Lucena Gómez. “Remarks on Gauge Invariance and First-class Constraints.” In: *Ann. U. Craiova Phys.* 21 (2011), S1–S10.
- [34] David J. Gross and Frank Wilczek. “Ultraviolet Behavior of Nonabelian Gauge Theories.” In: *Phys. Rev. Lett.* 30 (1973). Ed. by J. C. Taylor, pp. 1343–1346. DOI: [10.1103/PhysRevLett.30.1343](#).
- [35] H. David Politzer. “Reliable Perturbative Results for Strong Interactions?” In: *Phys. Rev. Lett.* 30 (1973). Ed. by J. C. Taylor, pp. 1346–1349. DOI: [10.1103/PhysRevLett.30.1346](#).
- [36] *Proceedings, Colloquium on Renormalization of Yang-Mills Fields, Marseille, June 19-23, 1972.* 1972.
- [37] William E. Caswell. “Asymptotic Behavior of Nonabelian Gauge Theories to Two Loop Order.” In: *Phys. Rev. Lett.* 33 (1974), p. 244. DOI: [10.1103/PhysRevLett.33.244](#).
- [38] D. R. T. Jones. “Two Loop Diagrams in Yang-Mills Theory.” In: *Nucl. Phys. B* 75 (1974), p. 531. DOI: [10.1016/0550-3213\(74\)90093-5](#).
- [39] E. Egorian and O. V. Tarasov. “Two Loop Renormalization of the QCD in an Arbitrary Gauge.” In: *Teor. Mat. Fiz.* 41 (1979), pp. 26–32.